Academic Year
2022 - 2023

Discovering seasonal differences in starlings using rs-fMRI

Silke Lemmens

Educational Commission Biomedical Sciences

Master Thesis in partial fulfilment of the requirements for the degree
Master of Biomedical Sciences: Neurosciences

Promotor(s)
Prof. dr. Marleen Verhoye

Co-promotor:
Dr. Jasmien Orije

Coach
Tamara Vasilkovska

Bio-imaging Lab, Campus Drie Eiken, building Uc. Universiteitsplein 1 2610 Antwerpen, Faculty of Pharmaceutical, Biomedical and Veterinary Sciences, University of Antwerp

University of Antwerp
Faculty of Pharmaceutical, Biomedical and Veterinary Sciences

Inhoud

1 Abstract

Starlings are open-ended learners that have the capacity to adjust their song every year. Song learning in this species is dependent on the photoperiod -the amount of light in a day, which causes them to switch from a photo-sensitive (winter); to a photo-stimulated (spring) and finally to a photorefractive state (late summer-fall). In the breeding season, the photo-stimulated period, male starlings will increase their song bout length and sing more often. Female starlings have periods of singing different from the males but will increase the amount of song when nest boxes are present. It has been previously shown with various modalities that the song control nuclei change size depending on the season, a phenomenon especially present in male starlings. These changes are one of the best-known examples of natural occurring neuroplasticity in adult animals. The underlying mechanism of neuroplasticity in humans or in animals is not completely understood. The starling is a good model to investigate these underlying mechanisms as they experience major neuroplasticity changes on a yearly basis. Neuroplasticity of this magnitude does not happen in humans, rodents, or other bird species such as the zebra finch, where major neuroplasticity occurs mostly early in life.

MRI is a great technique to perform longitudinal studies on animals or humans. It gives the opportunity to follow and manipulate the animals for a longer period without the need to sacrifice them during the experiment. Resting-state functional MRI (rs-fMRI) is a well-known technique in the neuro-imaging community to unravel networks present in the brain and to investigate the differences between certain groups. This MRI technique has been used for many years in humans and rodents, in birds however, only two studies are known up until today. This technique has not been done before in starlings. Therefore, we wanted to investigate whether rs-fMRI is a good technique to use in birds, specifically the starling. In this project, static rs-fMRI is used because we want to establish the basic functional connectivity networks, before moving on to more sophisticated, but less-established techniques like dynamic rs-fMRI. To extract functional connectivity, various analysis methods were applied. First, independent component analysis (ICA) was used to check whether there is any activity in the data that can be isolated. Second, region of interest (ROI)-based functional connectivity analysis was conducted, where based on the ICA outcomes pairwise connectivity between ROIs was calculated. This gives us an overview of the connectivity between two specified regions and the difference between the groups. Lastly, seed-based analysis is performed to investigate which voxels and thus brain regions are connected to a certain seed and the differences between groups as well. To use MRI data, an exclusion of non-neuronal signal is needed. This can be done using a low bandpass filter, quadratic detrending and global signal regression. Until today there is no consensus about whether global signal regression should be applied, and which method would remove all unnecessary signal while at the same time retaining the real neuronal signal. Therefore, we tested the analysis with and without removing the global signal from the data.

An overall finding from our experiment is that both sexes had increased functional connectivity during the breeding season compared to the non-breeding season. The song control nuclei (HVC-RA), which were previously known to change structurally in males, also change functionally in our resting-state data, which is an intriguing finding. We also notice that other seed areas fluctuate significantly between seasons, suggesting that plasticity exists outside of the well-known song control nuclei as well. Our project provides a starting point for deciphering the functional networks in the birdbrain, but more investigation is required to uncover unknown networks.

2 Abbreviations

A	Anterior
BOLD	Blood oxygen level dependent
CMM	Caudal medial mesopallium
CT	Computed Tomography
dHb	deoxygenated Haemoglobin
DLM	Dorso-lateral division of the medial thalamus
DVR	Dorso-ventral ridge
EPI	Echo-planar imaging
F_BS	Females breeding season
F_NBS	Females non-breeding season
FA	fractional anisotropy
FC	Functional connectivity
FDR	false discovery rate
fMRI	functional MRI
GE	Gradient Echo
GIFT	Group ICA of fMRI toolbox
GSR	global signal regression
HVC	used as a proper name (Higher Vocal Centre)
I	inferior
ICA	independent component analysis
Int	intermediate
L	left
LMAN	Lateral magnocellular nucleus of anterior nidopallium

LR	bilateral, left-right
M	Middle
M_BS	Males breeding season
M_NBS	Males non-breeding season
MLd	dorsal lateral nucleus of the mesencephalon
MRI	Magnetic Resonance Imaging
NCL	caudolateral nidopallium
NCM	Caudal medial nidopallium
Ov	Nucleus ovoidalis
oxyHb	oxygenated Haemoglobin
P	Posterior
PET	Positron Emission Tomography
PFC	prefrontal cortex
QDT	quadratic detrending
R	right
RA	robust nucleus of arcopallium
RF	Radiofrequency
ROI	Region of interest
Rs-fMRI	resting-state functional MRI
S	superior
SAM	Small Animal Monitoring
SBL	Song bout length
SCS	Song control system
SE	Spin Echo

SPECT	Single-Photon Emission Computed Tomography
SPM	Statistical Parametrical Mapping
TE	echo time
TR	repetition time
UV	ultraviolet

3 Introduction

3.1 Why are songbirds good models for vocal learning?

Songbirds are vocal learners that can be used to explore the mechanisms subserving learned vocal communication similar to human speech.[4] Vocal learning is the capacity to learn to produce new sounds for communication. Songbirds can be used for investigation of the neural substrate and socially sensitive neural circuitry for vocal learning. Other species, such as rodents, use vocalizations to communicate as well but are known as vocal non-learners as their behaviour is innate, not learned.[5]

3.1.1 Comparable pathways

A human brain and a bird brain have many differences. Birds don't have gyri such as humans to enlarge their brain surface. In humans, the corpus callosum connects the two hemispheres with each other. In birds, a corpus callosum is not present, the hemispheres are connected using an anterior and a posterior commissure.[6] The birdbrain consists of large subregions divided by white matter connections in lamina. These pallial subregions are: hyperpallium, mesopallium, nidopallium and the arcopallium. Despite the many differences between the brains of these two species, a few networks display some similarities.

A) Song learning pathways

Both humans and songbirds have specialized brain circuits that control learning and the production of speech and song, respectively. In songbirds, such as the starling, the song control system can be divided into two main pathways: the anterior pathway (figure1, white line) which controls vocal imitation and the posterior pathway (figure1, red line) that controls production of learned vocalizations.[1,7] The anterior forebrain pathway of the songbird consists of the Lateral magnocellular nucleus of anterior nidopallium (LMAN) in the pallium, Area X in the striatum and the dorso-lateral division of the medial thalamus (DLM) in the thalamus. This forms the pallial-basal ganglia-thalamo-pallial loop. Area X is suggested to induce stereotypy and LMAN induces variability into the songs and thus enables vocal imitation.[1,7] The posterior pathway, known as the song motor pathway, consists of the HVC (*used as a proper name*) and the robust nucleus of arcopallium (RA). HVC, which is functionally equivalent to Broca's area in humans[8], controls sequencing while the RA controls acoustic structure of syllables. The analogous human pathway for the anterior forebrain pathway is, the cortico-basal ganglia-thalamo-pallial loop, which involves Broca's area, the anterior striatum, and the anterior thalamus. The posterior song motor pathway is analogous to the laryngeal motor cortex.[1,7] In humans, Broca's area is responsible for language production and comprehension[9], Wernicke's area is known to process the sounds of speech and to store word meanings.[10] The thalamus works as a relay station for sensory information.[11] The comparison of the vocalization pathways between songbirds and humans is visualized in figure 1.

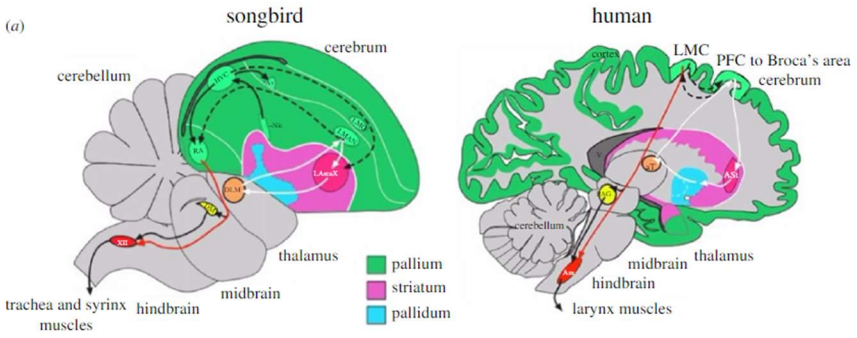

Figure 1: Visual representation of the comparability of the pathways for song learning and vocalization in the songbird brain vs the human brain.[1] Both have two main pathways: the anterior pathway (white line), which controls vocal imitation and the posterior pathway (red line), that controls production of learned vocalizations, and connections between both pathways are indicated by the black dotted line. Abbreviations explained in abbreviation list.

B) Auditory pathways

Similarities between songbirds and humans can also be found in the auditory pathway (figure 2). In both species sound vibrations are picked up by the inner ear hair cells, which synapse to sensory neurons.[12] Those project to the cochlea and lemniscal nuclei of the brainstem, which project to the inferior colliculus (humans) or the dorsal lateral nucleus of the mesencephalon (MLd) (birds) and to the thalamic auditory nuclei, medial geniculate body (humans) or nucleus ovoidalis (Ov) (birds). The thalamic nuclei make connections with the primary auditory cell populations in the pallium: layer 4/5 primary auditory cortex (humans) or L2 (birds). Layer 2 and 3 of the primary auditory cortex in humans are similar to avian L1 and L3 neurons.[12] The avian caudal medial nidopallium (NCM) and caudal medial mesopallium (CMM) are similar to layer 2/3 of the human auditory association cortex including Wernicke's region as they form reciprocal intrapallial connections and they both receive input from L2. The NCM is also involved in auditory memory.[8] The neurons of the RA cup could be similar to layer 5 and 6 of the human auditory association cortex, these send auditory feedback projections to thalamic and midbrain auditory nuclei.[12]

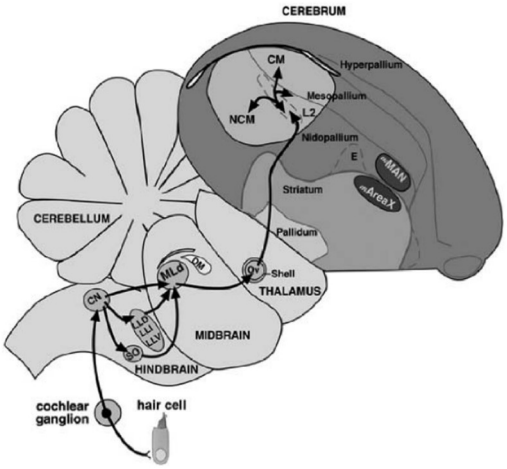

Figure 2: Visual representation of the auditory pathways in the songbird brain. The black line indicates the direction of the auditory pathway starting in the hair cells of the ear. The pathway ends in the secondary auditory nuclei. [13] Abbreviations explained in abbreviation list.

C) Lateralization

It is well-known that speech and language in humans are hemisphere specific. Broca's area and Wernicke's area are mostly active in the left hemisphere, especially in right handed people.[14] In zebra finches, there is also a left hemispheric dominance, where structural properties of some parts of the secondary auditory cortices, such as the left NCM, are predictive of future learning accuracy already during the sensory phase.[8-15] In other birds, such as pigeons and even starlings, hemispheric dominance has been shown in the hippocampus.[16] This indicates that the process of lateralization occurs similarly in birds and humans, which is remarkable given that these species were separated millions of years ago from a common ancestor.

3.2 Sturnus Vulgaris

The European starling (*Sturnus Vulgaris*) is a songbird where both males and females learn to sing in contrast to zebra finches, where only males sing. The reason for singing differs between male and female starlings and varies across seasons. Males, however, sing throughout the year with an increase in songs in the photo-stimulated period, which is the breeding season. In the breeding season, males mainly sing for mate attraction and direct their song towards females. Outside the breeding season, males sing less and not directed to females. This song is thought to serve dominance or territory maintenance.[17] Females sing from October until mid-April, mainly in the non-breeding season. It has also been shown that females sing more when they are occupying a nestbox.[18] Female starlings sing throughout the year, in the breeding season the function is thought to play a role in

intrasexual competition. Even though females are capable of singing complex songs, involving all categories of song, it is unclear whether all females sing or sing complex songs. The complexity of male song has also shown to be significantly higher than that of female song over all song measurements.[19]

The starling is an open-ended learner. They can adjust their song again every year before the next breeding season. It has been shown that starlings can even learn a new song after a year in full isolation[20]. This is in contrast with the canary, another open-ended songbird.[21] In general, song learning can be divided in three different stages: the first stage is the sensory phase, in which the birds are exposed to song by their social group and memorize it. The second stage is the sensorimotor phase which can be subdivided into two phases: first a subsong phase occurs during which the youngsters calibrate their vocal instrument and next there is a plastic song phase where the bird tries to match the song memorized in the sensory period. The third stage is crystallization, where the song has fully matured and after which a song cannot be changed anymore.[22,23] This last stage is present in all songbirds, but the duration differs between closed- and open-ended learners. In closed-ended learners, like zebra finches songs cannot be adapted after this phase. In open-ended learners such as starlings, the term crystallization means that the song does not change during the breeding season. Open-ended learners can restart the cycle and learn a new song each year, during in the non-breeding season.[24] In canaries, another open-ended learner, the song becomes unstable at the end of the breeding season. During fall, the plastic song becomes stable again, ready for the next breeding season.[24] Open-ended learners are capable of expanding their song repertoire with age.[24,25] Eens et al. showed that starlings seem to add more song types instead of overwriting the previous one as is the case in canaries.[24,25]

3.2.1 Starling Songs

Starlings have a large repertoire of songs (20-70 types) and are capable of learning heterospecific imitation; mimicry of heard sounds.[25] These birds are intermediate mimics, meaning that every bird incorporates several imitations in their song.[26] Starling song can be divided into three distinct classes, each with their typical function. Class 1 whistles are sung only by male starlings for long-distance vocal interactions, which aim for recognition and classification of populations and species. Class 2 whistles are produced by both sexes and can be shared by birds living together in captivity, while in the wild each whistle is unique to the bird. Class 3 song, warbling, is used by both sexes to communicate over a short distance. This song class does not elicit vocal interactions, in contrast with class 1. Class 3 songs consist of highly organized sequences, which start with individual motifs and at the end species-specific motifs, like clicks and high-pitched trills. As described above class 2 and the start of class 3 songs serve the function of individual recognition between birds.[27]

When starlings are kept in isolation, class 2 whistles fail to develop when the songs are only presented through loudspeakers.[28] Isolation also leads to atypical warbling (class 3) which lack the species-specific motifs at the end. This signifies that social experience is important to fully develop their natural song.[27]

3.2.2 Seasonal changes

Starlings are seasonal breeders, which means they have a circannual reproductive rhythm with periods of high reproductivity during the breeding season in spring. (See figure 3) This rhythm is dependent on the photoperiod – the amount of light per day. When daylight is less than 11.5h per day the photosensitive period is reached, making the birds responsive to longer day lengths. As days begin to lengthen during the photosensitive period, birds become photo-stimulated. During this period, also known as the breeding season, testes size increases, their song quality improves, and their song control nuclei almost double in size, known as the breeding season. When the photoperiod is long (>12h) for an extended period, the starlings enter the photorefractive state, their testes size decreases again and the birds go through molt. Only when the daylength decreases again, the photosensitive stage can be reached again.[29-30] In males, it has already been shown that the song control nuclei (HVC, RA) were structurally larger in the breeding season compared to the non-breeding season.[17]

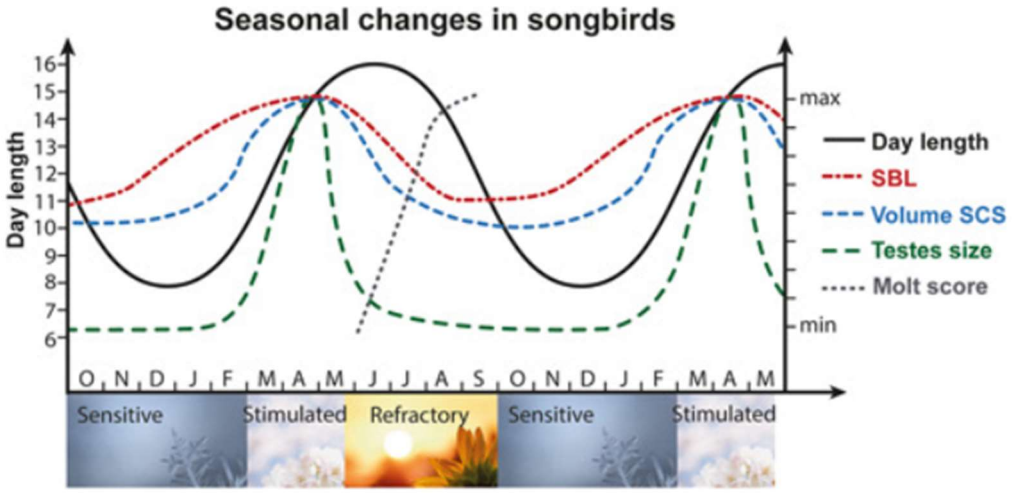

Figure 3: This figure shows the seasonal changes in male European starlings. Day length determines the reproductive rhythm, when it drops below 11.5h the photosensitive period is reached making them responsive to longer day lengths. These longer day lengths cause photo-stimulation which comes with an increase in testes size (green line), increased song bout length (SBL, red line) and an increased volume in the song control system (SCS, blue line). When the daylight is increased for a longer period, the birds become insensitive to light. Then they experience molting (losing feathers, grey line).[3]

3.3 Neuroplasticity

In general, the brain is a highly adaptable and dynamic organ that possesses the ability to form new connections, reorganize its structure or function in response to intrinsic or extrinsic stimuli, a phenomenon known as neuroplasticity.[31] This is most prominent during early childhood in humans and is essential for the development of crucial skills, including language and hearing. In contrast, the plasticity of these circuits decreases in adulthood, making it more challenging to master these skills. Critical or sensitive periods are periods of heightened neuroplasticity in life, but the brain can remain plastic during life.[32,33] During these periods, specific experiences are required to promote normal behaviour.[34] Impulse activity resulting from sensory experience activates the molecular cascades underlying plasticity.[35] Neural circuits are strengthened by Hebbian plasticity; when the presynaptic neuron is constantly activating the postsynaptic neuron, the synapse between the two is reinforced.[34]

A) Critical period
A critical period is a well-defined period of heightened sensitivity[32,33] during which specific skills, such as vision, hearing and language, are acquired. The critical period for first language syntax, for example, occurs within the first year of life.[36] During this period, sensory experience plays a crucial role in shaping the neural circuits involved in basic sensory processing. As the critical period ends, these skills can no longer be learned and the brain undergoes reorganization to accommodate other sensory modalities.[37,38] Early deprivation of auditory or visual input can result in a failure to develop the necessary neural circuits for processing sensory information.[33]An example is amblyopia or a lazy eye, where the treatment is only effective when performed during childhood.[39]

B) Sensitive period
Similarly, a sensitive period is a specific, not well-defined or reoccurring time during which neural circuits are highly susceptible to change. After this period a new skill can still be learned, however it will be more difficult.[40] Sensitive periods for lower order processes end earlier than for high-level circuits. For example, the sensitive period for language acquisition ends before the period required for social development.[34]

The concept of neuroplasticity and critical periods is supported by numerous studies. For example a study in non-human primates showed that deprivation of visual stimuli during the critical period can lead to nystagmus and behaviour similar to those observed in blind humans.[41] Similarly, language acquisition is another example of the sensitive period concept. Research has demonstrated that automatically acquiring a first language during

childhood is easier than learning a second language after puberty which is more difficult and requires more conscious effort.[32,33] Other studies have demonstrated that congenitally deaf children, for instance, lack auditory input which results in the reassignment of auditory regions to other senses.[37,38] Consequently, when cochlear implants are inserted after the critical period, patients may exhibit abnormal responses, such as altered auditory perception and language accuracy.[37,42] Conversely, research on congenitally deaf adults who use sign language have demonstrated activation of the auditory cortex, indicating that this region has been repurposed to support visual processing of language.[37]

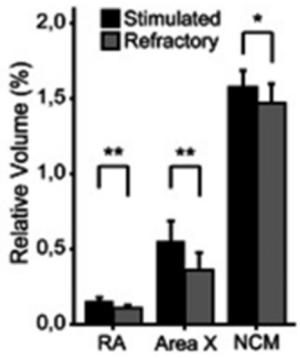

*Figure 4: Results of volume measurements on song control nuclei (RA, area X) and an auditory nucleus (NCM). The photo-stimulated period is the breeding season (black box), and the photo-refractory period is part of the non-breeding season (grey box). Significant results indicated by * p<0.05 and ** p<0.01.[3]*

It is well established that starlings also undergo neuroplasticity in adulthood. Seasonal plasticity has been partly investigated, mainly in the song control system, however the true functional differences in the songbird brain throughout the seasons are not well understood.[3] Previous studies in starlings have already shown structural differences between the seasons in the song control system and recently in other sensory systems. Figure 4 illustrates the volumetric changes measured *in vivo* using MRI in two main song control regions (RA and Area X), but also in the NCM which is part of the auditory system. These nuclei had a higher relative volume in the breeding season, the photo-stimulated period than in the non-breeding season, the photorefractory period. These differences show that there is plasticity in the starling brain.[3,43] Another study, shown in figure 5, shows the seasonal plasticity using tractography, an MRI technique, which shows the volume of the HVC-RA tract, which is part of the song control system.

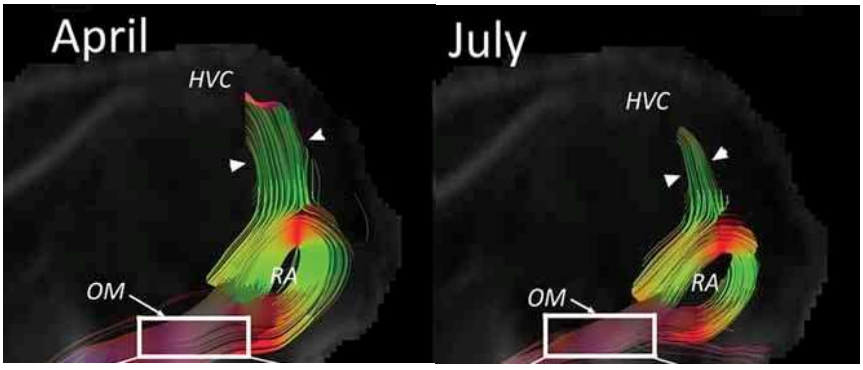

Figure 5: This figure shows a fiber tracking started from RA which has a connection with HVC. This tract is bigger in April, the breeding season, compared to July, the non-breeding season. This shows there is structural seasonal neuroplasticity in the song control system. OM = tractus occipitomesencephalicus, a fiber bundle leaving from the arcopallium. [2]

3.4 Imaging modalities

To further unravel the mechanisms of neuroplasticity in songbirds, we need appropriate tools. We chose magnetic resonance imaging (MRI), which is a non-invasive imaging technique and therefore can be used to perform longitudinal studies on the same subject. It uses electromagnetic waves unlike other imaging modalities that use ionizing radiation such as positron emission tomography (PET), single-photon emission computer tomography (SPECT) and computer tomography (CT).[42]

PET and SPECT use radioactive tracers to unravel functional activity, e.g., to visualize tumours. These techniques are capable of measuring plaque load, synaptic density, neuroinflammation and perfusion.[44,45] CT in contrast uses X-rays to investigate anatomical abnormalities such as kidney stones.[46-47] CT can also measure perfusion parameters on the capillary level of various tissue types.[48] MRI is versatile as it can measure biochemistry, functionality as well as structural properties of tissues without potentially harmful radiation.[49]

3.4.1 Principles of MRI

The principles of MRI start with a hydrogen atom present everywhere and in great amount in the human body, it contains one proton which spins around its axis. This creates a magnetic momentum. Under normal circumstances the direction of magnetic momentum is random in the body. When an external magnetic field is applied, these spins have either a spin-up (along the magnetic field, low energy state) or a spin-down (opposite of the magnetic field, high energy state). The spins will precess out of phase along the magnetic field with a certain frequency dependent on the magnitude of the field strength. The application of a radiofrequency (RF) pulse at the resonance frequency of the spins will cause a change in the distribution of the equilibrium of the spins and the spins will (partly) precess in phase. The in phase-precessing of the spins will induce an alternating magnetic flux which induces an electromotive force in a receiver RF coil, this is the MR signal.[50]

The spins will return to their equilibrium and dephase following two relaxation processes. In T1, spin-lattice relaxation, the environment or lattice absorbs the energy of the proton spin as they return to their equilibrium distribution. It is characterized as the time until 63% of thermal equilibrium is recovered. Water has a long T1 and thus looks dark on T1-weighted images, in contrast to fat. In T2, spin-spin relaxation, the spins mutually affect their 'magnetic field strength' causing fluctuations in their precession frequencies that leads to a decay in the signal. Water has a long T2 causing it to look bright on T2-weigthed images. Also, inhomogeneities in the external magnetic field influence the precession frequency leading to a faster T2* relaxation. The relaxation times are dependent on the tissue type and biochemical environment providing a tissue specific MRI contrast.[50-51]

3.4.2 Functional MRI (fMRI)

Functional MRI (fMRI) is a type of MRI used to investigate the function of certain brain regions. Changes in neural activity can be assessed via changes in the blood-oxygenation-level-dependent (BOLD) signal or via the measurement of tissue perfusion or blood-volume changes. This BOLD signal is based on the difference in magnetism between oxygenated haemoglobin (oxyHb, diamagnetic) and deoxygenated haemoglobin (dHB, paramagnetic). The latter causes an increased dephasing which attenuates the T2*-weighted signal. When a task is being performed, the active brain regions use more oxygen, leading to a localized increase in dHB. To ensure enough oxygen in the active regions, the local arterioles will dilate causing an increase in local blood flow and an excess of oxyHb. This will result in an increase of the ratio oxyHb/dHb leading to a higher BOLD signal (figure 6).[52] This signal can be used to study the entire network of brain areas that are engaged in a task while a subject is performing it or to investigate functional networks during rest.[53] When interpreting the results of BOLD signals, vascular and metabolic subcomponents should be taken into account since the observed BOLD signal change is dependent on cerebral blood flow, cerebral blood volume and the oxygen metabolism.[52] There is a delay (≈3-5s) between receiving a stimulus and the actual metabolic response/measured BOLD peak. The haemodynamic response function couples neural activity with the fMRI signal and shows this delay in signal.[53-55]

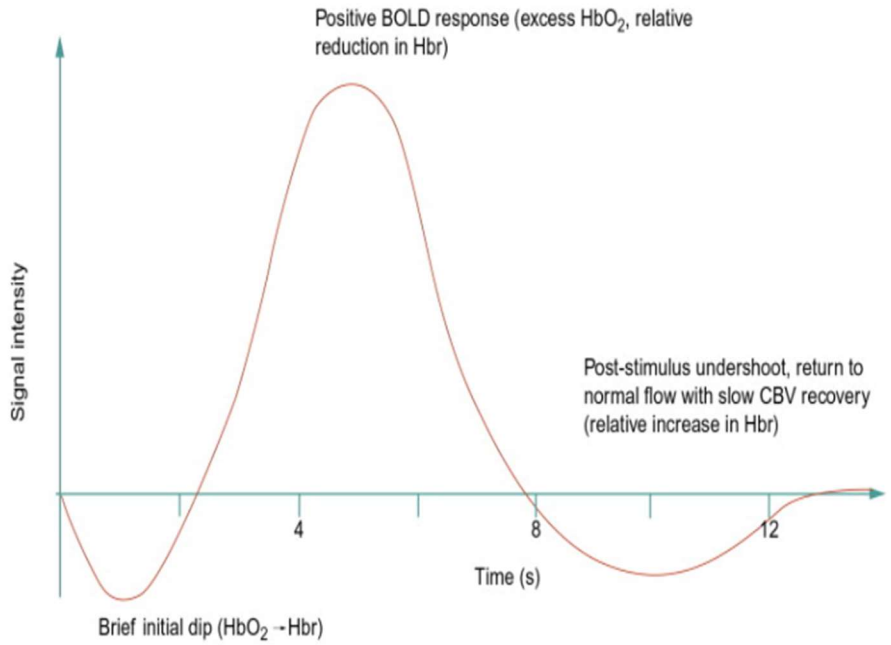

Figure 6: This figure shows the haemodynamic response function. The BOLD signal will first dip when the brain is using more oxygen. When the vessels dilate, there will be an increase of oxygenated haemoglobin, this will give a positive BOLD response because this changes the ratio of oxyHb/dHb. In this figure OxyHb = HbO_2 and dHb= Hbr [56]

fMRI has a relatively high spatio-temporal resolution, though several things have to be taken into consideration.[53] A first consideration is that it measures a surrogate signal, BOLD, whose spatial specificity depends on the used sequence. Researchers can choose between a T2*-weighted gradient echo sequence, which is more sensitive to both target signal and noise/distortions and a T2*-weighted spin echo sequence, which allows for higher specificity.[57] Echo-planar imaging (EPI) is a fast MRI technique with which you can use a gradient or spin echo sequence. In single-shot EPI the entire image is taken at a single excitation. The advantage thereof is reduced imaging time and decreased motion artifacts. Acquisition of an image only takes 20-100 ms. Using the multi-shot EPI, a higher spatial resolution can be obtained with less distortions, comparable to conventional MRI. In spin-echo pulse sequences each line of image data is collected during a repetition time (TR) period. The total imaging time will thus depend on the amount of lines/phase-encoding steps. In EPI, multiple lines of image data are acquired during a single TR.[58] When using multi-shot EPI, a portion of the k-space is acquired in each shot until a complete image is taken.[58]

Another consideration is that animals need to be immobilized to avoid movement artifacts, although some studies have explored function in awake animals.[59,60] However, very often anaesthesia is used. Special care should be taken when selecting an anaesthetic as different anaesthetics can have various known effects on brain function and/or brain vasculature that should be taken into account.[61] There is no one anaesthetic that is best for fMRI, the choice will depend on the type of experiment you want to do. However, several things are known about the effects of anaesthetic agents. The most widely used ones are medetomidine and isoflurane. It has already been shown that medetomidine, an injectable anaesthetic, is associated with a reduced strength and occurrence of interhemispheric connectivity between homotopic regions. Isoflurane is an inhalation anaesthetic and thus easy for induction as well as maintenance of anaesthesia, but the amplitude of the signal is dependent on the dose. It also induces vasodilation resulting in slower and weaker haemodynamic responses for stimulation. Another inhalational anaesthetic is sevoflurane, which maintains cerebral autoregulation better.[62] With careful selection of experimental parameters, this technique allows studying of spatial location, possible hemispheric lateralization, magnitude and time course of BOLD contrast changes across different stages.[42]

The signal acquired with fMRI is used to calculate functional connectivity (FC). When two regions show similar activation patterns using fMRI, the regions are said to be functionally connected with each other. The networks

that can be derived from this method are those used in controllable tasks, such as the visual, auditory and motor networks. These networks can also be found in resting-state fMRI. Rs-fMRI can unravel functionally connected networks when the brain is at rest.[63]

3.4.3 Resting-state fMRI (rs-fMRI)

Resting-state fMRI (rs-fMRI) captures the activation when the brain is at rest, which reflects the distinct network systems in the brain.[64] It is interesting to study resting-state networks because the brain consumes 20 % of the total energy and 60-80% of this is used as inherent activity for communication between neurons and their supporting cells.[65-66] Functionally connected networks at rest are patterns of low-frequency fluctuations that can be discovered by rs-fMRI.[67] This technique is already a well-established method in the field of neuro-imaging. Many studies have already successfully analyzed resting-state networks in rodents, non-human primates[68-70] and some have even accomplished it in birds. All these studies were performed using anaesthesia.[60,71] In humans, rs-fMRI has also already been validated, these studies are carried out in awake humans.[72] This technique has thus been validated to use in different species and to unravel the functional networks present in the starling.

Rs-fMRI can be subdivided into two main branches: static and dynamic rs-fMRI. The static technique only looks at functional interactions, stationary in space and time. The dynamic technique assumes that FC across networks changes over time. It represents transient and recurring patterns over time, this can reveal neural mechanisms not found in static rs-fMRI.[73] However, static rs-fMRI is a well-established technique in rodents and humans and would be the first step to investigate FC in a new species or model.

3.5 Networks in the songbird brain

Using rs-fMRI, functional networks can be investigated. The networks that appear in rs-fMRI are known to have intrinsic FC, which is thought to occur mainly at frequencies below 0.1 Hz. Above this threshold, fluctuations in the signal are thought to belong to non-neuronal causes such as cardiac rhythm.[67] This intrinsic activity can be used to investigate the brain's organization into large-scale functional networks.[63]

Diffusion MRI and histological preparations have already been used to unravel structural networks in bird. These networks are expected to be functionally connected as well and thus retrievable in rs-fMRI. Besides the auditory system and the song control system discussed earlier, other known networks in the songbird brain are discussed below.

The dorsal ventricular ridge (DVR) is the avian sensory system which consists of a visual part, an auditory part, and a trigeminal part. The wulst comprises most of the hyperpallium, with anteriorly somatosensory functions and posteriorly visual functions.[74]

Visual information goes from the retina to the nucleus rotundus of the thalamus.[75] The primary visual system in the avian forebrain consists of the entopallium, nidopallium intermedium and the mesopallium dorsale. From the entopallium connections go to the striatum/basal ganglia. From the nidopallium intermedium the connections go to associative and motor areas.[76] By injecting biocytin in the entopallium, a connection with the mesopallium ventrale was revealed, which successively projects to mesopallium dorsale and nidopallium intermediale. This information is then transmitted to the caudolateral nidopallium (NCL) and the arcopallium, which is a part of the motor pathway.[74]

The avian homolog of the prefrontal cortex (PFC) is thought to be NCL as it is an integration center that connects sensory input to limbic and motor structures. It contains many dopaminergic fibers analogous to the human PFC. NCL is responsible for decision making, rule tracking, encoding of subjective values and association.[76] In crows, associative learning has shown to activate the striatum and the amygdala.[75]

4 Research questions

Starlings are a good model for vocal learning and have already shown to experience structural neuroplasticity in the breeding season versus the non-breeding season, but little is known about the functional changes upon learning over these seasons. Therefore, we want to use an *in vivo* method like rs-fMRI to:

1) Evaluate whether rs-fMRI is a good modality to investigate FC in starlings

   Since rs-fMRI has not been done often in birds and especially not in the starling or any open-ended learner in general, we want to evaluate whether this technique can be used in this species. By our knowledge rs-fMRI has only been performed on two bird species: the zebra finch and the pigeon.[77,78] Rs-fMRI is a well-established method in other species, such as in humans and rodents. Therefore, we hypothesize that this technique is feasible in starlings and that we will find FC even though there is no previous knowledge about what functional networks to expect.

2) Evaluate whether the functional networks in the starling brain change seasonally.

   In this project, starlings are used to investigate the difference in FC between seasons. Starlings are known to behave differently and have changes in their songs in the breeding season compared to the non-breeding season. Also, structural differences between the seasons have been established in starlings.[2] This raises the question whether there are also differences in FC and mainly in functional networks in the starling brain over the seasons. The well-established method of static rs-fMRI is used in this project to investigate these networks and the seasonal differences in the starling.

   We hypothesize that the FC in the breeding season will be higher compared to the non-breeding season in both sexes. Both sexes sing, although for different reasons, so it is expected that both experience plasticity. As structural plasticity has already been shown, although mainly in males, we expect higher connectivity in the breeding season. *Orije et al. 2020* showed that injecting testosterone in female starlings increases the fractional anisotropy value of the HVC-RA tract. In male starlings the testes size and thus testosterone production increases in the breeding season, explaining a possible factor in seasonal neuroplasticity and the increase in volume in certain regions during the breeding season.[79] This indicates that even though plasticity occurs in females, we would expect more differences between the seasons in the males. Females differ in singing behaviour from the males. Only larger females sing, during part of the photosensitive phase, the non-breeding season and part of the photo-stimulated phase, the breeding season in contrast to the males who sing all year but especially during the breeding season.[18]

   As there is no corpus callosum in starlings and lateralization has previously been observed in zebra finches for the auditory nucleus and in pigeons and starlings for the hippocampus, we hypothesize that the connections will be distinct in both hemispheres.[15,16]

5 Material and methods

5.1 Experimental set-up

In this study, 28 European starlings were used (15 males and 13 females). They were kept in aviaries inside with a light-cycle matching their natural photoperiods. In the aviary, water and food is given ad libitum. The birds were scanned in an MRI scanner (Pharmascan 70/16 US, 7 T, Bruker, Ettlingen, Germany) in the breeding season (March-April) and non-breeding season (October). Prior to and during scanning the starlings were anaesthetised using a 0.3 ml intramuscular injection of a mixture containing 10 ml medetomidine (Domitor, Pfizer) and 0.25 ml ketamine (Anesketine, Eurovet). This mixture is continuously administered throughout the scan using an intramuscular catheter at 0.12 ml/h. During the scan, temperature and breathing rate are monitored respectively by a cloacal probe and a pressure sensitive pad. The monitoring is done by Small Animal Monitoring (SAM) software. The body temperature of the starling is kept at 41.5°C using a warm air feedback heating system. When the measurements are done, the anaesthetics are reversed using an intramuscular injection of 1.5 ml atipamezole (Antisedan, Pfizer). The birds are placed in a recovery cage underneath an infrared light, and as soon as they are fully recovered, they return to the group aviary. All procedures are done in accordance with the European guidelines for the use of laboratory animals and approved by the Committee on Animal Care and Use at the University of Antwerp, Belgium (86/609/EEC).

5.2 Acquisition

Resting-state fMRI is acquired on a 7 T Biospec scanner with a linear transmit volume coil and a parallel receiver surface array. Three orthogonal T2-weigthed Turbo RARE images with 15 slices of 1 mm were acquired with a TR of 2500 ms and an echo time (TE) of 33 ms. These images are used for a consistent positioning of the rs-fMRI slice package. The rs-fMRI data is acquired using two different methods: single shot Gradient Echo-EPI and single shot Spin Echo-EPI. In this project only Gradient Echo-EPI data will be used as this is the most sensitive technique. They both have a TR of 2000 ms and a TE of 10 ms for Gradient Echo-EPI and 16 ms for Spin Echo-EPI. 13 axial slices were acquired with a slice thickness of 0.8 mm and an interslice distance of 0.1 mm. A field of view of 3x3 cm^2, a matrix size of 128x96 and a bandwidth of 400 kHz were chosen. 150 repetitions were acquired for each bird. This results in a measuring time of five minutes.

5.3 Processing

Pre-processing is carried out with Statistical Parametric Mapping (SPM). First, the images are realigned to the first image, using a least squares approach and a six-parameter spatial transformation. After that, the images are normalized to a single subject using a least square method to enable comparison between animals. These realigned images are repositioned to match the images of a chosen reference bird. Subsequently, in plane smoothing is done using a Gaussian kernel with a Full Width at Half Maximum of (0.468 x 0.638) mm. The data is filtered (filt) using a low band pass filter of 0.005-0.08 Hz, similar to the filtering performed in an experiment from Behroozi et al. Filtering is a necessary step to exclude signal that does not originate from neuronal activation. It is expected that the neuronally generated haemodynamic signals do not cross 0.1 Hz, however, there can still be some non-neuronal signal in below this frequency.[80] The chosen range is assumed to contain all neuronal information with minimal additional noise.

Besides filtering, we also performed Quadratic Detrending (QDT) and Global Signal Regression (GSR). Until now there is no consensus about which method is the most scientifically correct, therefore we proceed with both methods. Detrending is an operation to remove a trend which is an intrinsically fitted monotonic function.[81] When a trend is removed, only the actual signal is left, then you can look at the true variability in the data without the trend. These trends can be caused by various non-neuronal factors. Detrending is necessary for enhancement

of classification accuracy when acquiring long scans. Many different types of detrending exist such as linear and quadratic. The use depends on the trend in the data.[82] GSR is the removal of signal variations present in every brain voxel, this can be useful as global signal is associated with head movement, respiration, and cardiac rhythms. One consideration to take into account when using GSR is that due to the mathematical manipulations, negative correlations are introduced. This makes the interpretation of GSR data hard as it is not known whether the interactions are actually inhibitory or a result of mathematics. Another consideration to take into account is that this signal could contain neuronal information and could be associated with arousal.[83-84]

The graph below (figure 7) shows the signal intensity over the repetitions for the original data, filt, filt_QDT and filt_QDT_GSR data. This clearly shows the impact of the techniques on the data, the purple line shows the original data. After filtering, the signal intensity is lower, when we zoom in on the lower intensities, the differences between filt, QDT and GSR becomes more clear. For GSR (yellow line), the peaks disappear, which doesn't happen using QDT. We can also see that the difference between filtered data and QDT data is not so big for most repetitions. This is an argument to perform the analysis only with QDT and GSR. From now on QDT data will be referred to as non-GSR data.

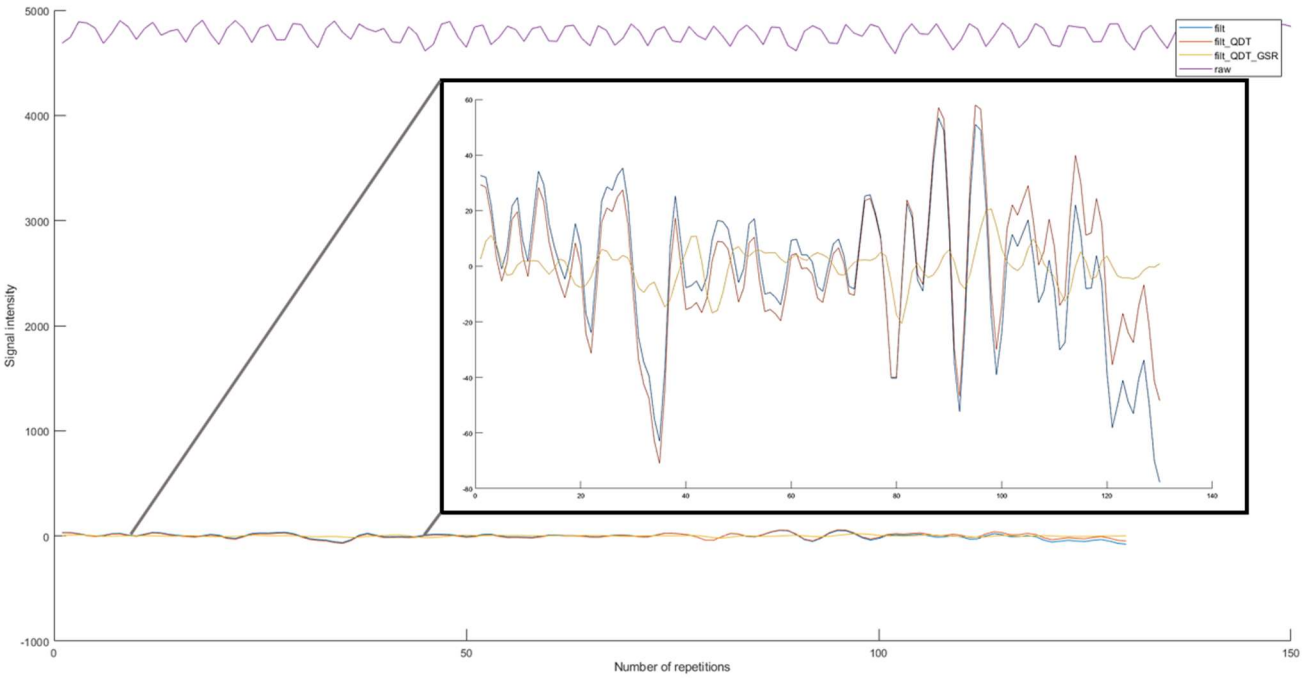

Figure 7: Example of effect of filt, QDT and GSR. The purple line shows unfiltered data, the blue one filtered only, the red one filtered + QDT and the yellow line shows data that is filtered, Quadratic Detrended and where the global signal is regressed.

To analyse FC, we perform Independent Component Analysis (ICA) using GIFT (Group ICA of fMRI toolbox) in MATLAB. It analyses group data in three steps. Firstly, a data reduction is performed with a concatenation of data in groups, afterwards group ICA is done with the Infomax algorithm. Finally a back reconstruction to single subject independent components and time courses is done.[85] When the components are generated, we match the activations with the corresponding brain regions, using an in-house made starling atlas in AMIRA (figure 8).

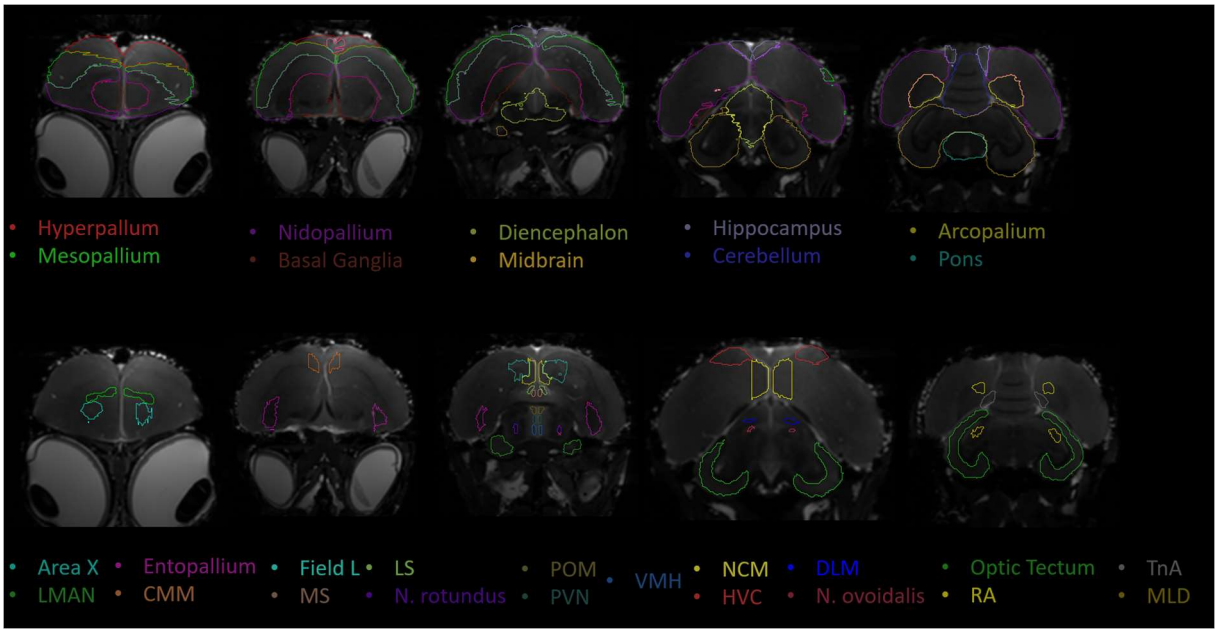

Figure 8: This figure shows a render of the atlas images in AMIRA showing all the regions and nuclei in the starling brain. The upper row shows the regions, and the lower row shows the known nuclei in the brain.[86] The name of the region is written in the colour of the atlas delineation itself.

Components were generated for the four different groups separately (Females-Breeding (F_BS), Females-Non Breeding (F_NBS), Males-breeding (M_BS), Males-Non Breeding (M_NBS)) and for all groups pooled together to explore what regions are activated during resting-state in the starling. As not much is known about rs-fMRI in birds, not to mention starlings, we compared the connectivity using 25 and 15 Independent Components. In theory when less components are used, more networks can be found. However, too little components will not give useful information either because all networks would be merged together. A good balance needs to be found. However, we found that more biologically relevant regions were present when 25 ICA's were used compared to 15, we therefore proceeded with 25.

We applied a data driven approach by using the components from the 25 ICA's to create parcellations in ITK-SNAP for further analysis. The most intense part of the component signifies the center of the functional activation, these were taken to delineate the regions. In total 37 regions were delineated. The regions were further specified using abbreviations for location terms; Anterior (A), middle (M), posterior(P) to indicate the place in the brain and superior (S), intermediate (Int), inferior (I) to indicate the depth. The hemisphere is indicated using left (L), right(R) or bilateral (LR). (See figure 9) This is done because many components comprised the same overarching region, for example the nidopallium.

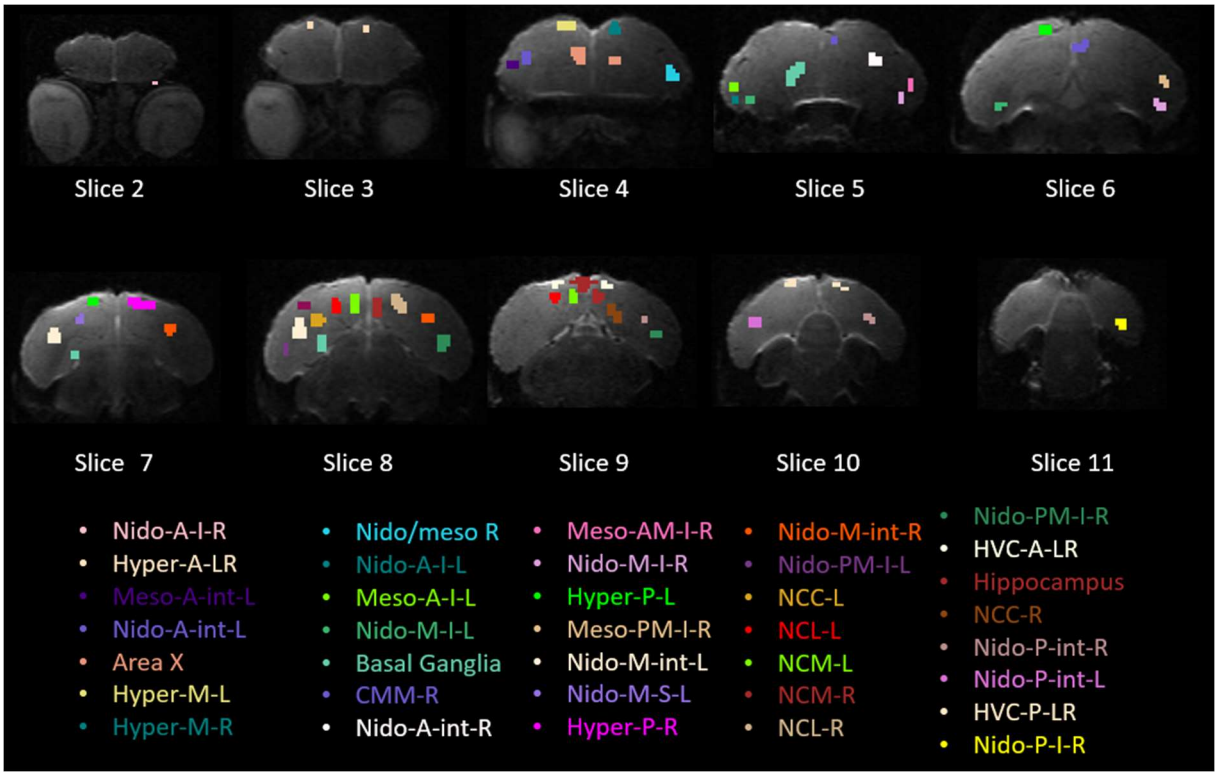

Figure 9: Overview of parcellations made based on the ICA component results. The brain is shown front to back. Nidopallium (nido), Hyperpallium (hyper), Mesopallium (meso). Anterior (A), middle (M), posterior(P) to indicate the place in the brain and superior (S), intermediate (Int), inferior (I) to indicate the depth. The hemisphere is indicated using left (L), right(R) or bilateral (LR). NCL = caudolateral nidopallium, NCM = caudomedial nidopallium, NCC = central caudal nidopallium, CMM = caudomedial mesopallium. The colours of the regions corresponds with the colours of the region names.

The ICA-based parcellations are used to investigate functional connectivity using FC matrices, these are created using an in-house script in MATLAB. FC-matrices are made for every group (M_BS, M_NBS, F_BS, F_NBS) and compared visually as well as statistically. These are matrices that are calculated by performing a Pearson correlation between the timeseries for each ROI. The values in the matrix present z-scores, which are the correlation values adjusted to a normally distributed scale. The comparisons were made between the breeding season and the non-breeding season. Statistically, we performed a two-sample T-test using the in-house made rs-fMRI pipeline in MATLAB, including a multiple testing correction, False Discovery Rate (FDR).

Apart from FC matrices, another way to explore FC is seed-based analysis. For this we need seeds of 4 voxels. We used the same regions as previously determined for the FC matrices. Here we reduced the amount of regions to the most biologically relevant ones, leading to a total of 15 seeds (figure 10). With these seeds, connectivity maps can be calculated. The analysis is performed using an in-house rs-fMRI pipeline in MATLAB. To start, we carry out a first level analysis on subject-level by performing a one-sample T-test by calculating the correlations between the timeseries of the mean BOLD signal of the seed voxels and all the other voxels in the brain, showing the connections to the seed for each subject. Next, a first level analysis per group is done. This includes a voxel-based one-sample T-test, which shows the t-value of the connections per group. From these maps, masks are created in xjview (MATLAB toolbox) with a cluster size of minimum 10 voxels and an FDR corrected P-value < 0.05. We merged the masks of the groups that we want to compare. These merged masks are used in the second-level analysis, where the seed-based connectivity maps of two groups are compared using a voxel-based two-sample T-test. The results of this analysis are statistical difference maps showing where the significant differences in FC between the two groups can be found. These significant difference maps are corrected using FDR ($p<0.05$).

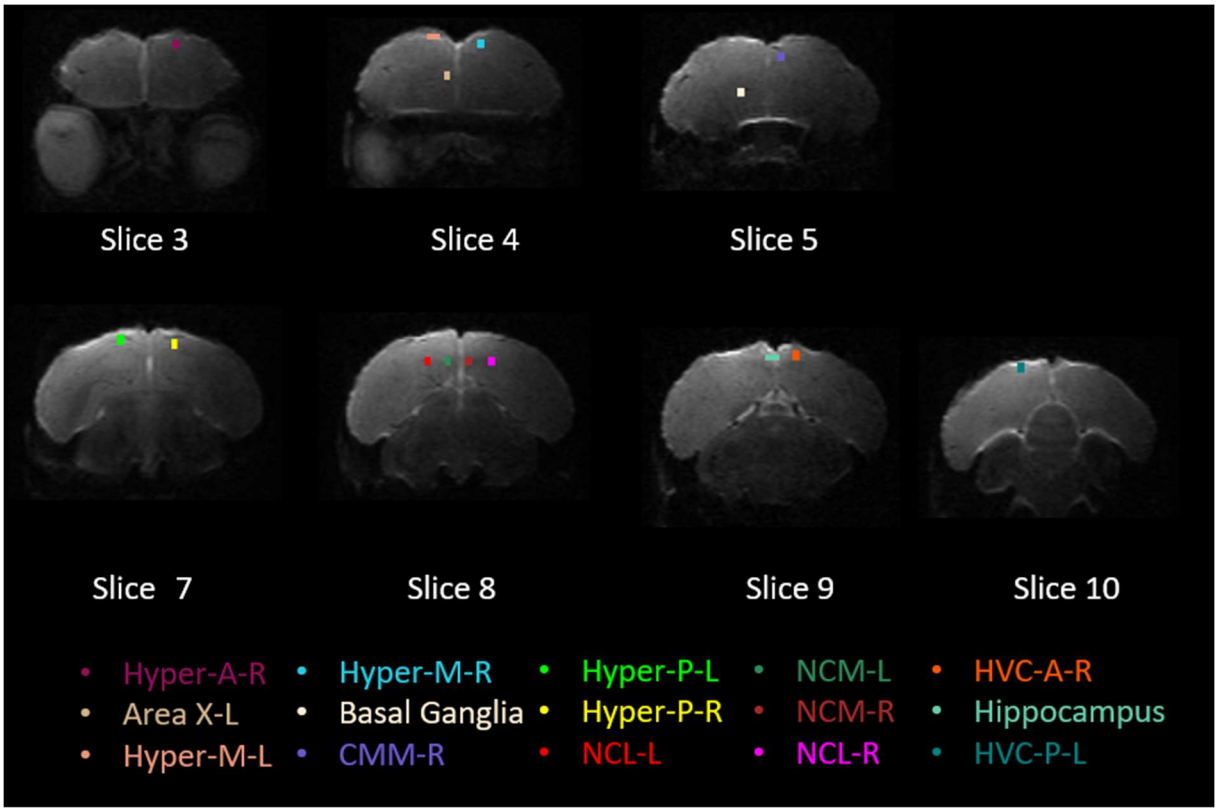

Figure 10: This figure shows the seeds used in the seed-based analysis, based on parcellations for FC matrices. The seeds are chosen based on the reduced FC matrices. Nidopallium (nido), Hyperpallium (hyper), Mesopallium (meso). Anterior (A), middle (M), posterior(P) to indicate the place in the brain and superior (S), intermediate (Int), inferior (I) to indicate the depth. The hemisphere is indicated using left (L) or right(R). NCL = caudolateral nidopallium, NCM = caudomedial nidopallium, NCC = central caudal nidopallium, CMM = caudomedial mesopallium. The colour of the seed corresponds with the colour of the seed name.

6 Results

The results section contains data from 15 male starlings in both seasons, 13 females in the non-breeding season and 11 females in the breeding season. All birds were scanned in both seasons so they could be their own control, however, two females were excluded due to problems in the pre-processing steps.

6.1 Independent Component Analysis (ICA)

The difference between 15 vs 25 components is mainly seen in the disappearance of biologically interesting structures such as HVC, Entopallium and CMM. Not necessarily more networks are seen when we use 15 components. They consist of spread-out pallial regions, instead of clear networks such as for example the auditory network. The components are usually a unilateral region instead of clusters in both hemispheres. Therefore, we concluded that 25 components was the best option to perform data driven analysis on biologically relevant regions.

ICA analysis for 25 components of the four groups is performed separately and once for all the groups pooled together to increase statistical significance. The components rendered by the pooled data are (Supplementary figure 1):

- NCM bilateral
- NCL bilateral

- Area X + LMAN
- Basal ganglia
- Hippocampus
- CMM
- Various regions of the pallia (Nidopallium, Mesopallium, Hyperpallium)

In all groups and the pooled data no noise components were found overall. Some different components were found when calculating the ICA's for the groups separately. Area X is only present in M_BS and M_NBS, Arcopallium in M_BS, Basal ganglia in F_BS and F_NBS, Entopallium in F_BS.

A two-sample T-test on the groups is done using the pooled data to investigate the differences between the seasons. Here no significant differences survive FDR correction ($p<0.05$).

6.2 Functional Connectivity matrices

6.2.1 Non-GSR matrices

The parcellations made based on the ICA data are shown in figure 9 above. The regions were clustered per system. The matrices show z-transformed scores of a pairwise Pearson correlation between the timeseries of each ROI. The colour bar of the matrices varies per technique (non-GSR and GSR) as they are based on the average minimum and maximum values from all the groups, a red colour indicates a high connectivity and a blue colour indicates a low connectivity or even anti-correlation.

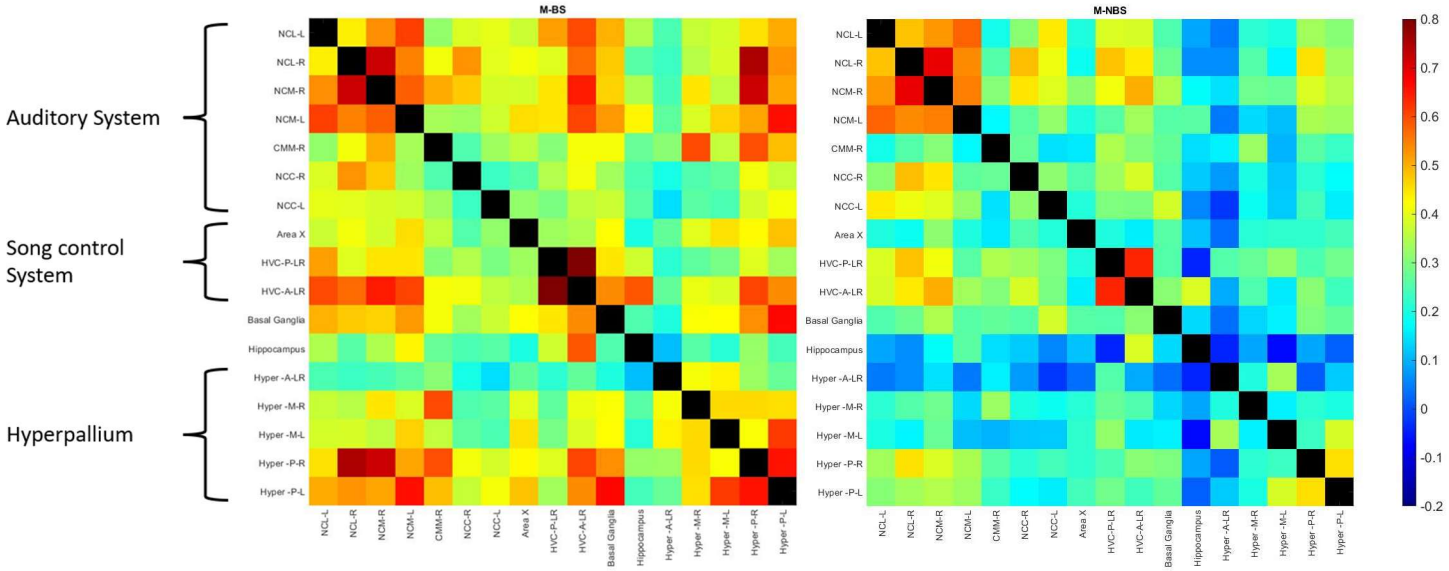

Figure 1111: Reduced ROI-based FC matrix showing mean z-transformed correlations without GSR for M_BS (left), M_NBS (right). Warm colours (red/orange) show positive or strong connections while colder colours (blue) represent less strong or anti-correlated connections. In this figure, a visual difference can be found between both seasons, where the FC matrix in the breeding season colours more yellow-red compared to the more green-blue FC matrix in the non-breeding season.

The complete matrices with 37 regions can be found in supplementary figure 2 for non-GSR data and supplementary figure 3 for GSR data. The matrices were reduced as no significant differences were observed (two-sample T-test, FDR correction, $p<0.05$). Since, when the number of comparisons is reduced, multiple comparison correction becomes less stringent, the first 15 regions are kept as these are the most biologically relevant. When we look at the matrices in figure 11, we can already see in M_BS that there is a strong connection between NCM-R and NCL-R, the posterior and anterior HVC and between the Hyper-P-R and the NCL-R and NCM-R. The first two are also visually present in M_NBS. When looking at both seasons, there seems to be a higher

connectivity in the breeding season compared to the non-breeding season. However, when performing a two-sample T-test on these matrices, no significant differences were found (FDR corrected, p<0.05). (figure 12)

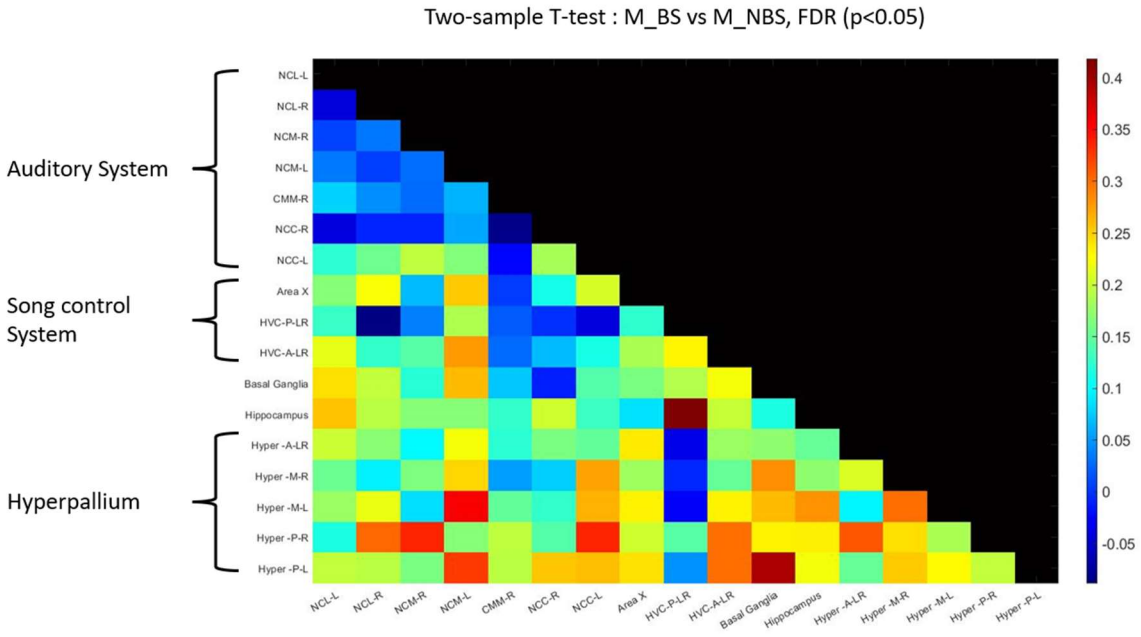

Figure 1212: Reduced ROI-based FC difference matrix showing the difference in z-scores of a two-sample T-test without GSR for M_BS vs M_NBS with FDR correction (p<0.05). Any significant differences are shown by a white square in the upper half of the matrix and by a white asterix in the lower half of the matrix. Warm colours (red/orange) show positive or strong connections, while colder colours (blue) represent less strong or anti-correlated connections. In this figure, no significant difference can be found between both seasons.

When evaluating the same matrix without multiple comparison correction we find the following matrix (figure 13). As no significant results were found (FDR corrected, p<0.05), maybe because of variation in the data or because there is no actual difference between the groups, we should be careful drawing conclusions from of this matrix. However, since this is the first time rs-fMRI has been performed on starlings, we are unsure about what to expect. Thus, we could use the uncorrected data as a starting point.

The uncorrected matrix shows mainly connections with hyperpallial regions and the hippocampus. Some of these connections are with NCM and NCL but also CMM and HVC. The differences in connections are different for the left and the right hemisphere.

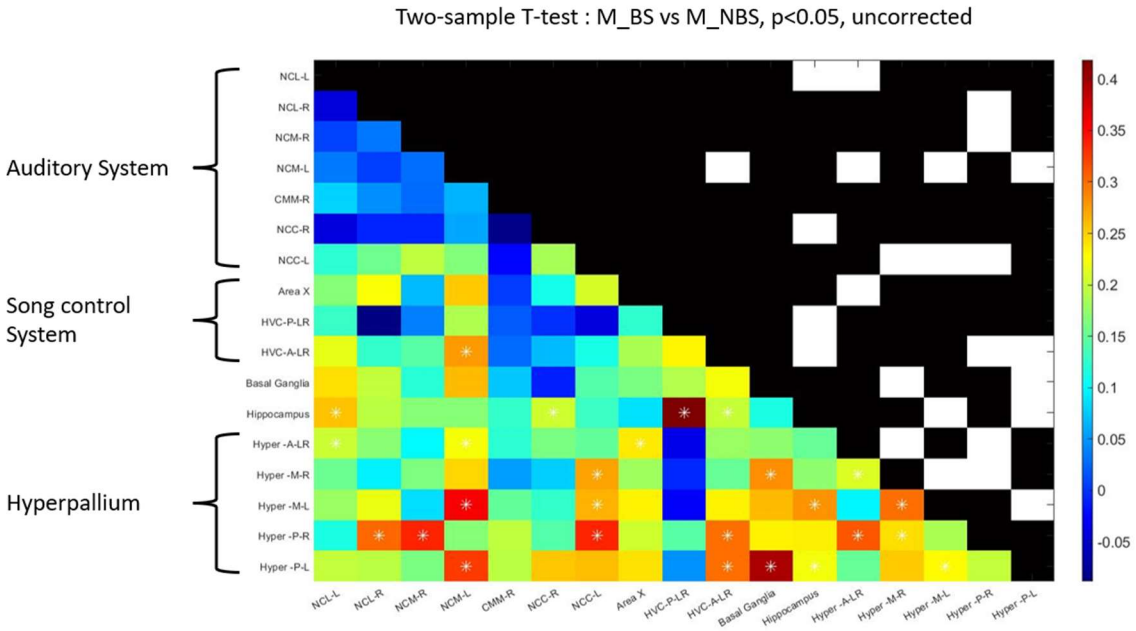

Figure 13: Reduced ROI-based FC difference matrix showing z-scores of a two-sample T-test without GSR for M_BS vs M_NBS with p<0.05, uncorrected. Any significant differences are shown by a white square in the upper half of the matrix and by a white asterix in the lower half of the matrix. Warm colours (red/orange) show positive or strong connections while colder colours (blue) represent less strong or anti-correlated connections. Several significant differences can be found between both seasons, mainly in the hippocampus and hyperpallial regions.

The same FC matrices are also created for the female starlings. These results can be seen in figure 14-16. Again, visually there seems to be a difference between the breeding season and the non-breeding season, where the FC matrix in the breeding season colours more yellow-red compared to the more green-blue FC matrix in the non-breeding season.

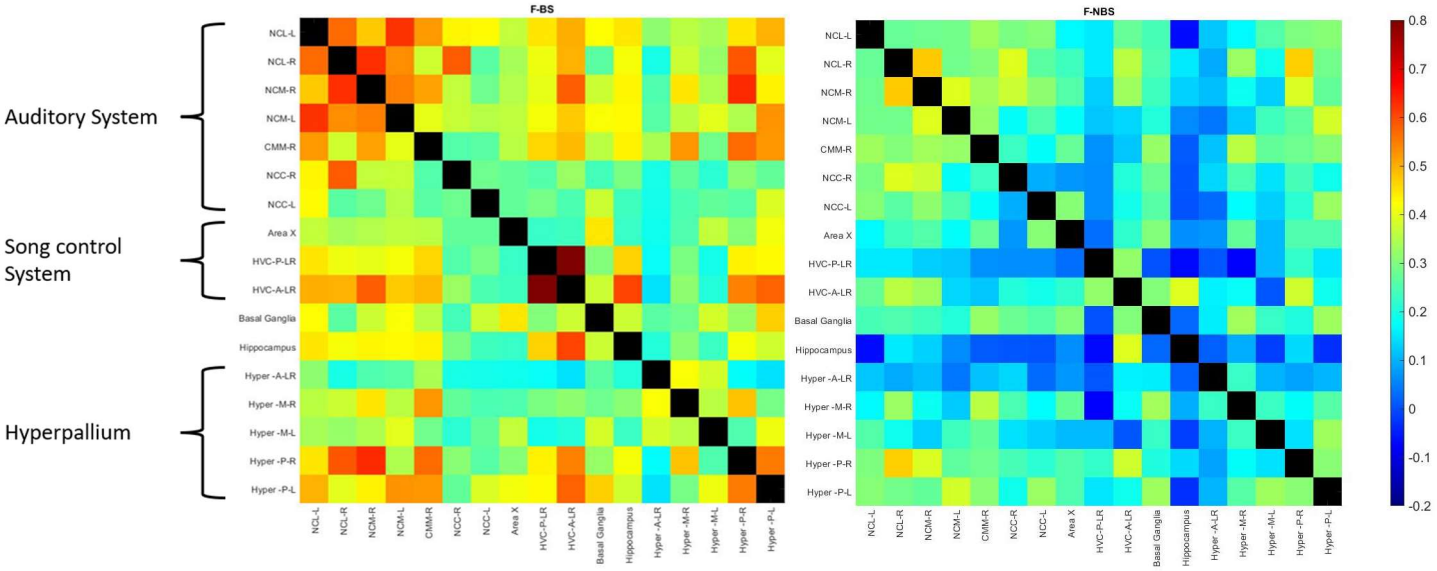

Figure 14: Reduced ROI-based FC matrix showing mean z-transformed correlations without GSR for F_BS (left) and F_NBS (right). Warm colours (red/orange) show positive or strong connections while colder colours (blue) represent less strong or anti-correlated connections. In this figure a visual difference can be found between both seasons, where the FC matrix in the breeding season colours more yellow-red compared to the more green-blue FC matrix in the non-breeding season.

For the females, two-sample T-tests are performed as well, with and without FDR correction. These results can be seen below in figure 15 and 16 respectively.

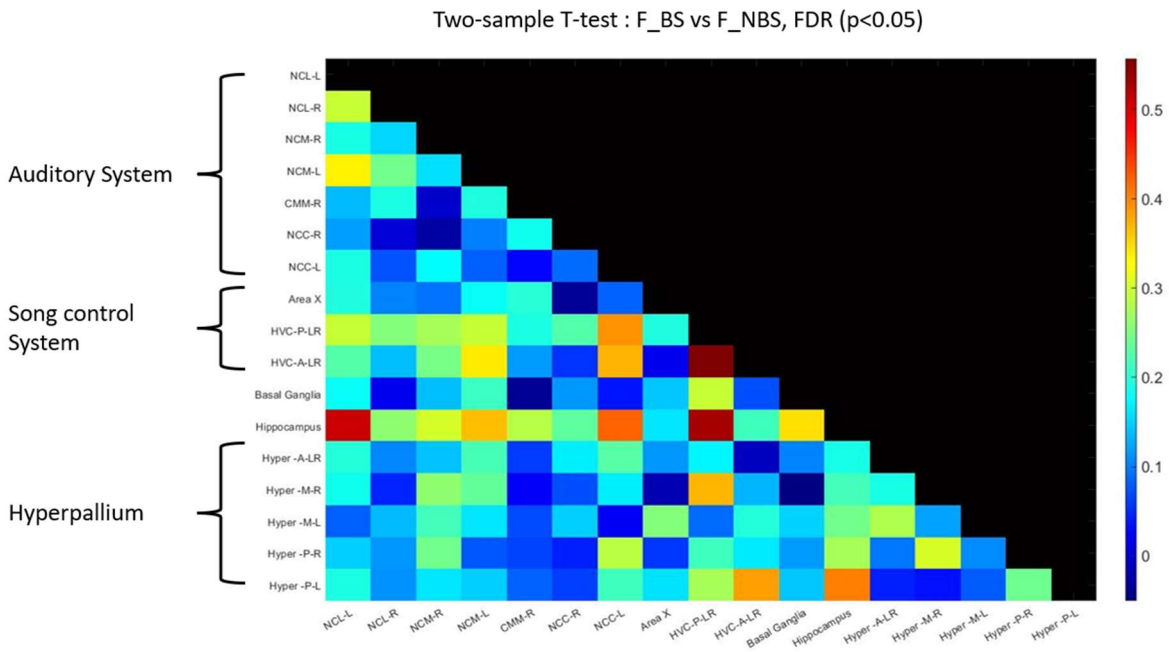

Figure 15: Reduced ROI-based FC difference matrix showing the difference in z-scores of a two-sample T-test without GSR for F_BS vs F_NBS with FDR correction (p<0.05). Any significant differences are shown by a white square in the upper half of the matrix and by a white asterix in the lower half of the matrix. Warm colours (red/orange) show positive or strong connections while colder colours (blue) represent less strong or anti-correlated connections. In this figure no significant difference can be found between both seasons.

No significant differences were found (FDR corrected, p<0.05). This would mean there is no difference for the females between the seasons. However, when looking at the uncorrected matrix, some potential differences appear.

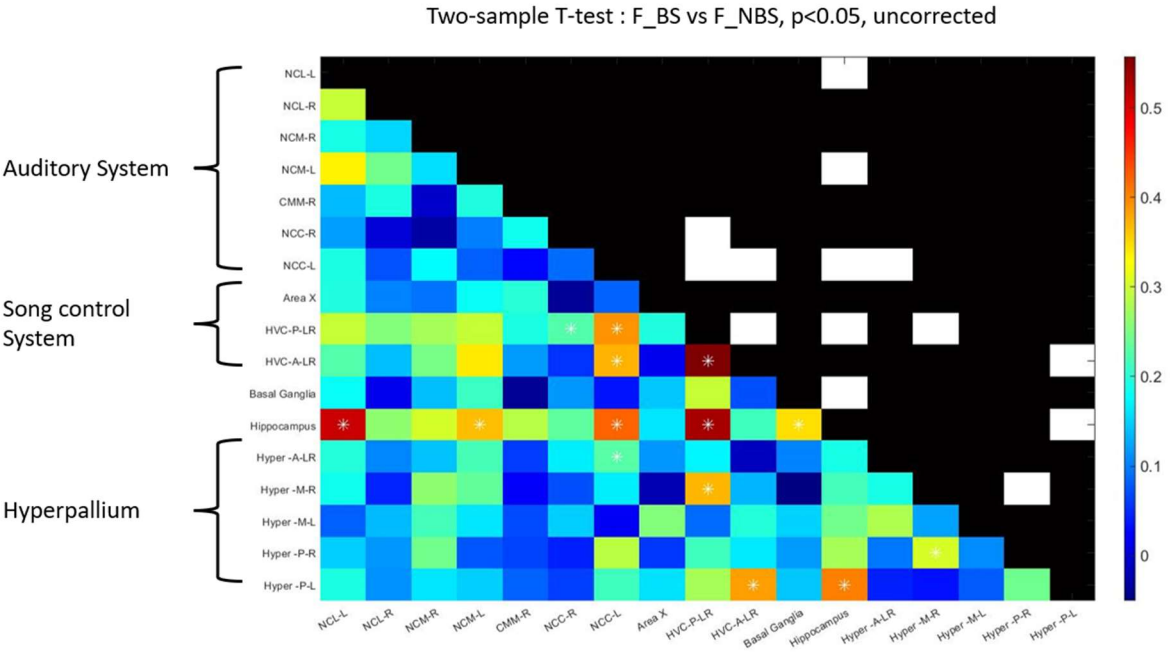

Figure 16: Reduced ROI-based FC difference matrix showing z-scores of a two-sample T-test without GSR for F_BS vs F_NBS with p<0.05, uncorrected. Any significant differences are shown by a white square in the upper half of the matrix and by a white asterix in the lower half of the matrix. Warm colours (red/orange) show positive or strong connections while colder

colours (blue) represent less strong or anti-correlated connections. In this figure several significant differences can be found between both seasons, mainly in the hippocampus, hyperpallial regions and the HVC.

In the uncorrected difference matrix, we see that many regions are differently connected to the hippocampus in the breeding and non-breeding season. Besides that, the NCC is more connected to both parts of the HVC during the breeding season. Both HVC's are more connected to each other as well, the posterior one is also connected to the hippocampus and hyper-M-R. The anterior HVC has a connection to Hyper-P-L. The differences in connections are different for the left and the right hemisphere.

When comparing the uncorrected, non-GSR matrices for both sexes, some similarities are found. The similar connections are: NCL-L with Hippocampus, HVC-P-LR with Hippocampus, HVC-A-LR with Hyper-P-L, Hippocampus with Hyper-P-L and Hyper-M-R with Hyper-P-R. The fact that these differences are found significant in both sexes, might be an indication that the differences are real and not false positive results.

6.2.2 Comparison with or without GSR

Since there is no consensus about whether GSR is the most correct way to handle resting-state data, we decided to perform every analysis with and without GSR. Before deciding this, we compared both modalities in difference matrices for every group (figure 17,18).

M_BS non-GSR vs GSR

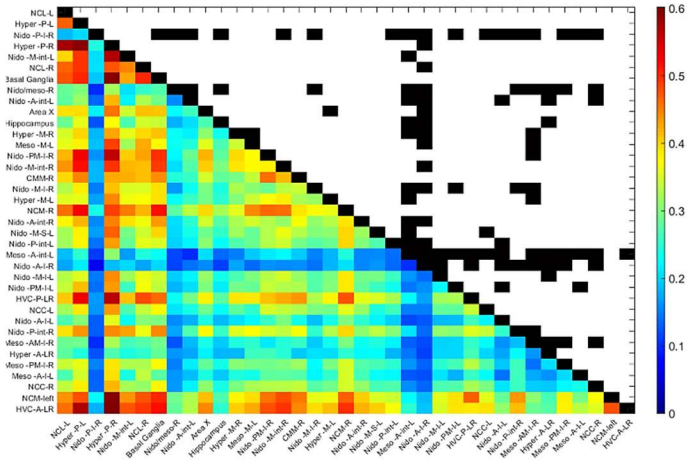

M_NBS non-GSR vs GSR

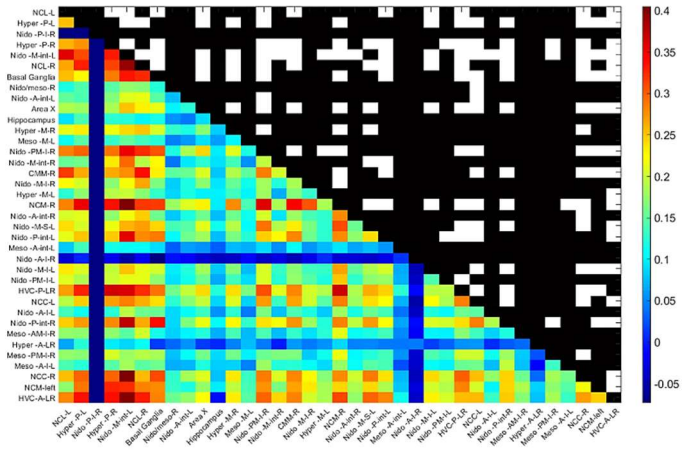

Figure 17: Unsorted difference matrix from a Two-sample T-test M_BS_non-GSR vs M_BS_GSR, FDR correction (p<0.05) (left) vs Two-sample T-test M_NBS_non-GSR vs M_NBS_GSR, FDR correction (p<0.05) (right). Any significant differences are indicated by a white square in the upper half of the matrix. Warm colours (red/orange) show positive or strong connections while colder colours (blue) represent less strong or anti-correlated connections. In this figure significant difference can be found between both modalities for the males. The differences are present in both seasons although less in the non-breeding season.

F_BS non-GSR vs GSR **F_NBS non-GSR vs GSR**

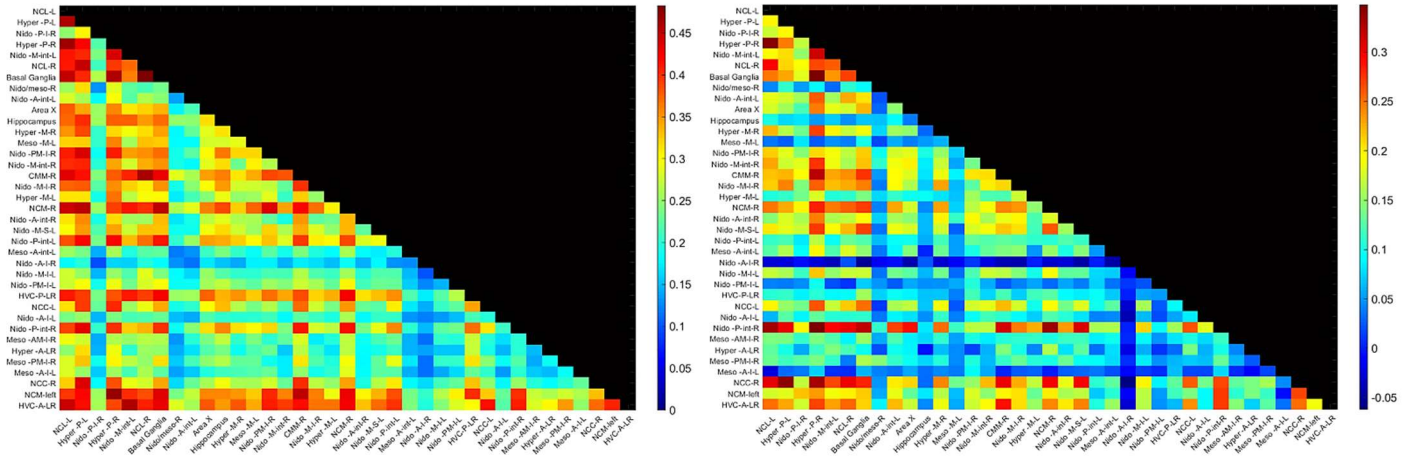

Figure 18: Unsorted difference matrix from a Two-sample T-test F_BS_non-GSR vs F_BS_GSR, FDR correction (p<0.05) (left) vs Two-sample T-test F_NBS_non-GSR vs F_NBS_GSR, FDR correction (p<0.05) (right). Any significant differences are shown by a white square in the upper half of the matrix. Warm colours (red/orange) show positive or strong connections while colder colours (blue) represent less strong or anti-correlated connections. In this figure, no significant difference can be found between both modalities for the females.

The above matrices show that GSR does have a significant effect on the FC for the males compared to non-GSR. For the females, on the other hand, no significant difference in FC can be found between the two methods. The difference for the males is especially prominent in the breeding season as the FC for almost every connection is significantly different with FDR correction (p<0.05). Because there are differences between both measures, every analysis is performed with and without global signal regression. The FC matrices below show the first GSR data.

6.2.3 GSR matrices

The FC matrices with GSR for the males (figure 19) look opposite of the non-GSR FC matrices (figure 11). The upper left corner of the matrix is more connected in the non-breeding season (right) compared to the breeding season. Overall, less connection is seen using GSR compared to non-GSR data.

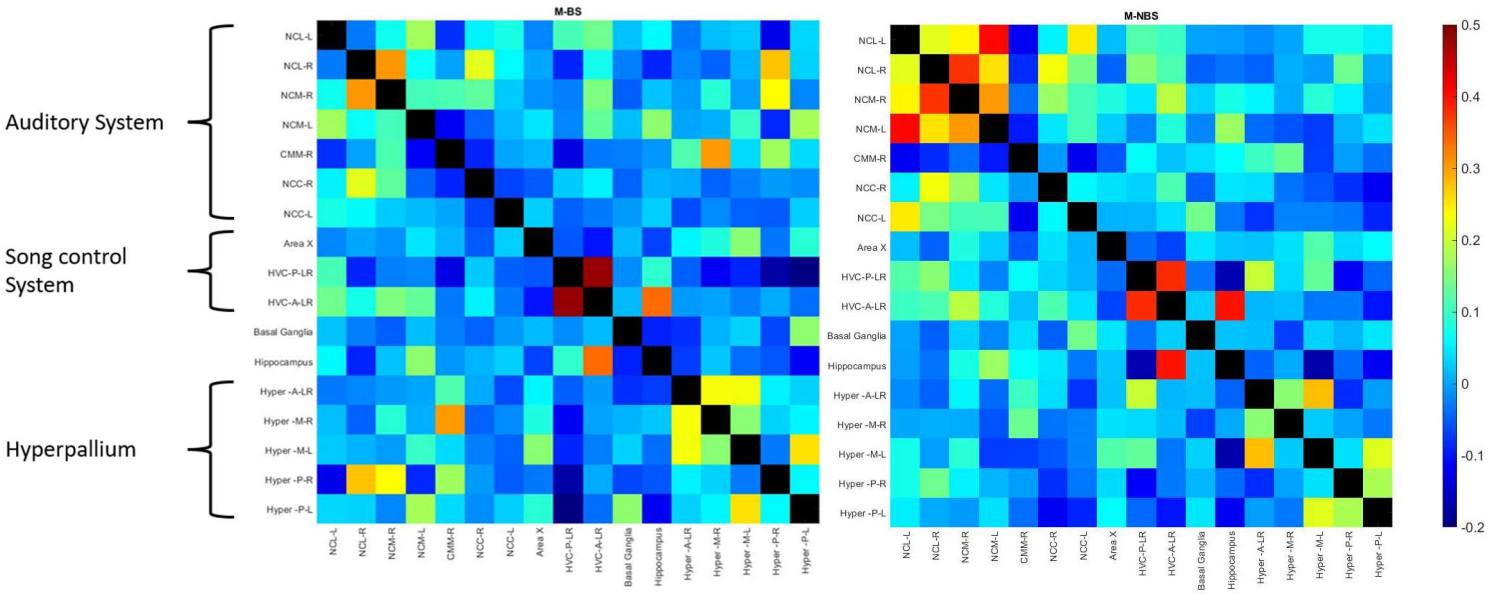

Figure 19: Reduced ROI-based FC matrix showing mean z-transformed correlations with GSR for M_BS (left) and M_NBS (right). Warm colours (red/orange) show positive or strong connections while colder colours (blue) represent less strong or anti-correlated connections. In this figure, a visual difference can be found between both seasons, with more connection in the non-breeding season.

In the two-sample T-test with FDR correction comparing both seasons in males one connection survives, HVC-P-LR with Hyper-A-LR (figure 20). This connection is higher in the non-breeding season compared to the breeding season. No other significant differences were found (FDR corrected, p<0.05).

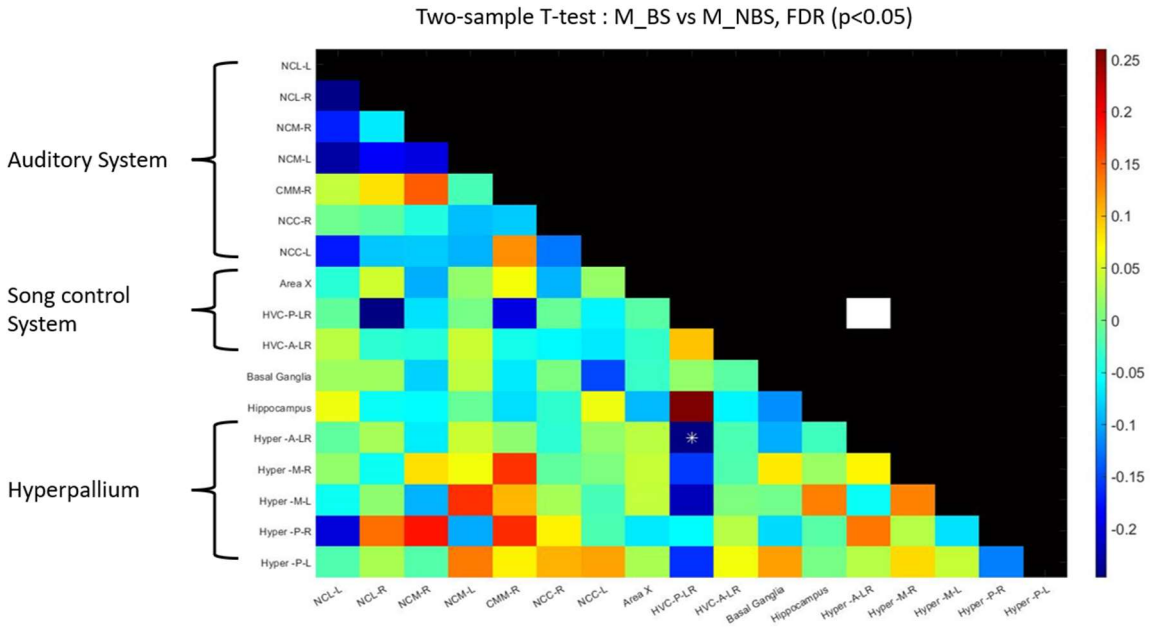

Figure 20: Reduced ROI-based FC difference matrix showing z-scores of a two-sample T-test with GSR for M_BS vs M_NBS with FDR correction (p<0.05). Any significant differences are shown by a white square in the upper half of the matrix and by a white asterix in the lower half of the matrix. Warm colours (red/orange) show positive or strong connections while colder colours (blue) represent less strong or anti-correlated connections. In this figure one significant difference can be found between both seasons, HVC-P-LR with Hyper-A-LR.

When looking at the uncorrected matrix more significant FC differences are present, including connections with NCL, HVC and the hyperpallium (figure 21). The differences in connections are different for the left and the right hemisphere.

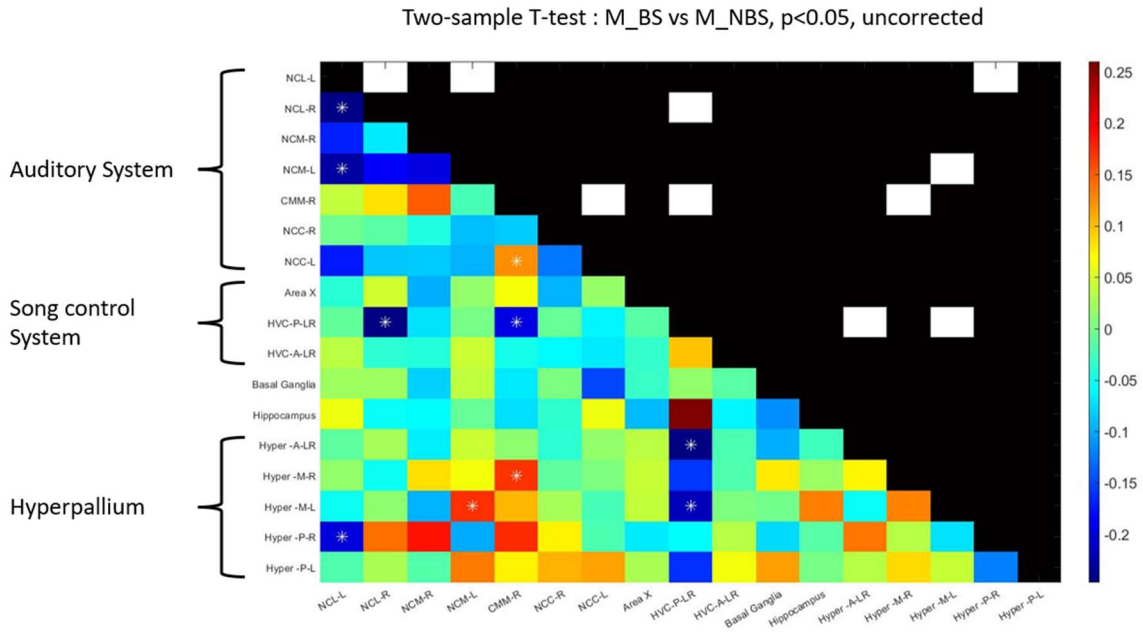

Figure 21: Reduced ROI-based FC difference matrix showing z-scores of a two-sample T-test with GSR for M_BS vs M_NBS p<0.05, uncorrected. Any significant differences are shown by a white square in the upper half of the matrix and by a white asterix in the lower half of the matrix. Warm colours (red/orange) show positive or strong connections while colder colours (blue) represent less strong or anti-correlated connections. In this figure several significant differences can be found between both seasons.

For the females, not many seasonal differences are seen visually. Only the connection between NCC-R and NCL-R and the connection NCM-L and NCL-L seem to really differ between the seasons (figure 22).

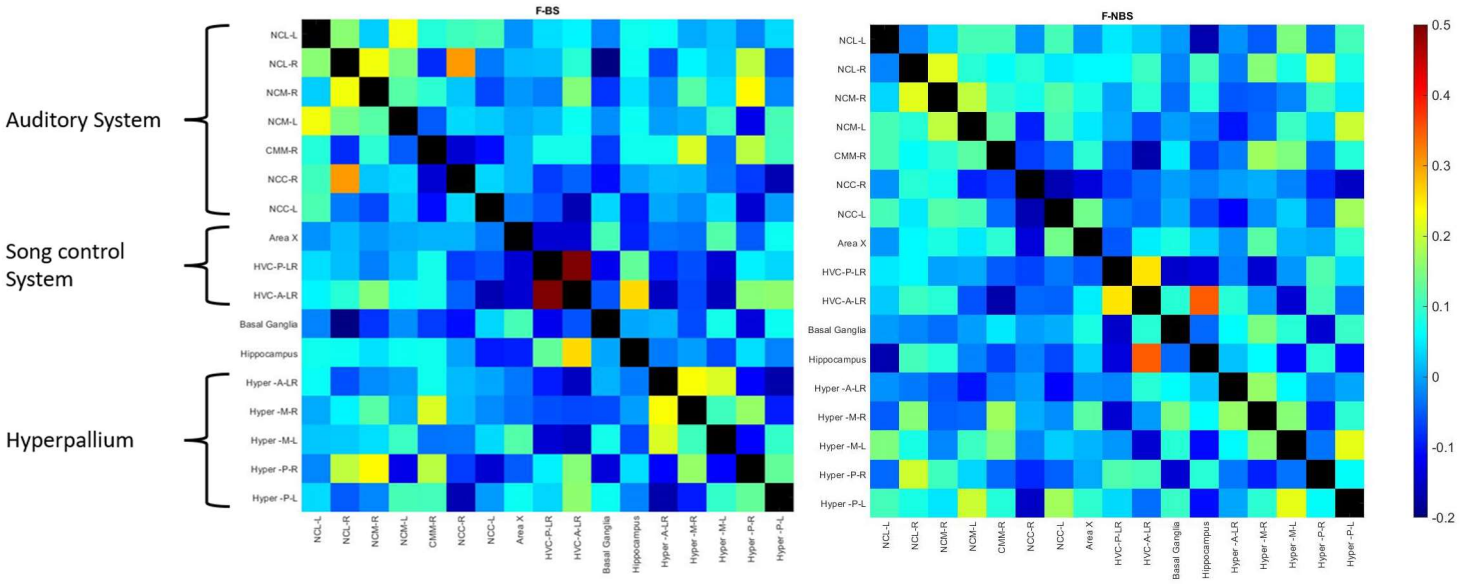

Figure 22: Reduced ROI-based FC matrix showing mean z-transformed correlations with GSR for F_BS (left) and F_NBS (right). Warm colours (red/orange) show positive or strong connections while colder colours (blue) represent less strong or anti-correlated connections. In this figure a no real visual difference can be found between both seasons.

Two-sample T-tests were carried out again with and without FDR correction, with correction no significant differences were found (figure 23).

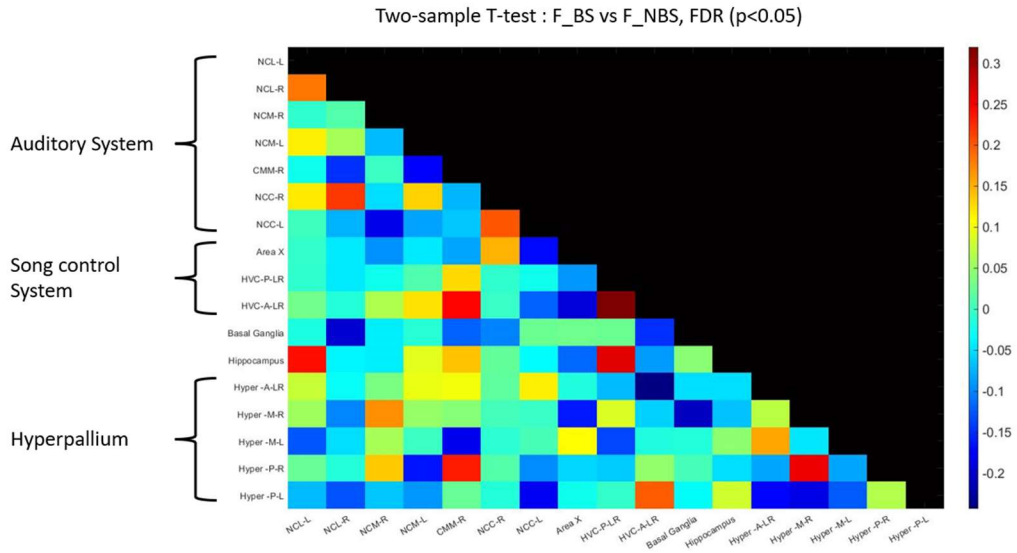

Figure 23: Reduced ROI-based FC difference matrix showing the difference in z-scores of a two-sample T-test with GSR for F_BS vs F_NBS with FDR correction (p<0.05). Any significant differences are shown by a white square in the upper half of the matrix and by a white asterix in the lower half of the matrix. Warm colours (red/orange) show positive or strong connections while colder colours (blue) represent less strong or anti-correlated connections. In this figure no significant difference can be found between both seasons.

In the uncorrected matrix (figure 24), we see differences in connections in NCL, Area X, HVC, hippocampus, NCC and the hyperpallium. The differences in connections are different for the left and the right hemisphere.

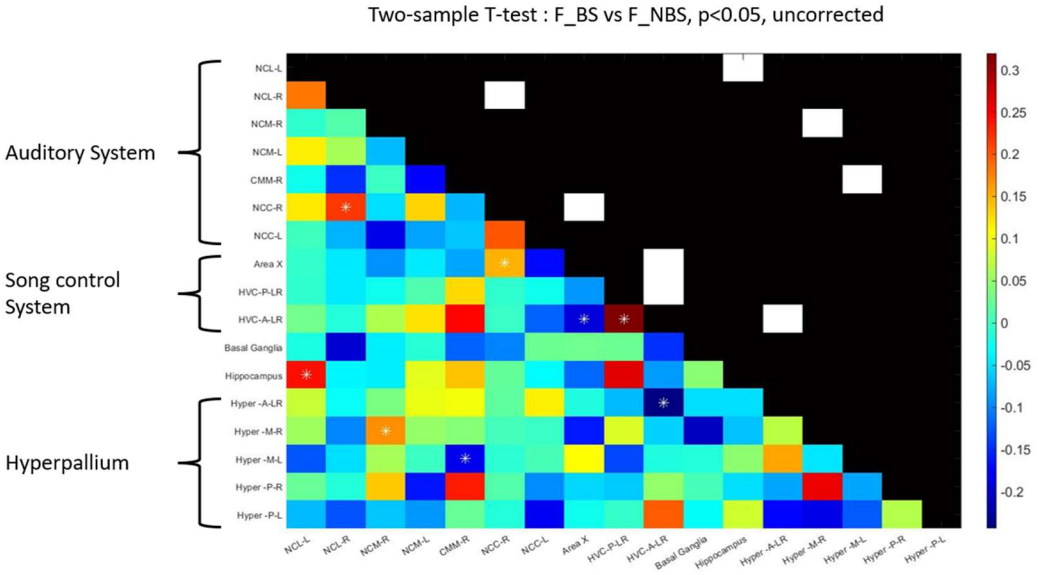

Figure 24: Reduced ROI-based FC difference matrix showing the difference in z-scores of a two-sample T-test with GSR for F_BS vs F_NBS p<0.05, uncorrected. Any significant differences are shown by a white square in the upper half of the matrix and by a white asterix in the lower half of the matrix. Warm colours (red/orange) show positive or strong connections while colder colours (blue) represent less strong or anti-correlated connections. In this figure several significant differences can be found between both seasons.

When comparing the uncorrected, GSR matrices for both sexes, no similarities are found among the significant differences.

6.3 Seed-based analysis

The seed-based analysis is performed using the four voxel seeds of 15 regions (figure 10), based on the reduced FC matrices. The analysis is performed with and without GSR. Not for all seeds significant results were found. For the detrended data, FDR-corrected significant results were only found in following seeds for the females: the basal ganglia, HVC-A-R, Hyper-A-R and Hyper-M-L. For the males, a significant difference was only found in HVC-P-L. For both sexes the FC is higher in the breeding season compared to the non-breeding season. When performing GSR, differences were found in FC for Hyper-M-L for the females and HVC-A-R and Hyper-P-R for the males. Over the two modalities, only one difference survives FDR correction in both, the Hyper-M-L. All of the seed regions are unilateral, the outcome is not replicated on the other side of the brain.

6.3.1 Results non-GSR

The results of the first level group level analysis for F_BS and F_NBS are shown on the left side of figure 25, a voxel-based one-sample T-map is created, showing the connectivity of the brain voxels to the voxels of the seed. On the right side, the second-level analysis is shown, which are the results of the voxel-based two-sample T-test, presenting voxels that demonstrate a significantly higher FC to the seeds in the breeding season. In this case the connection is stronger in the breeding season compared to the non-breeding season. The seed can be seen in the first two columns as the red most dot in the group-level analysis.

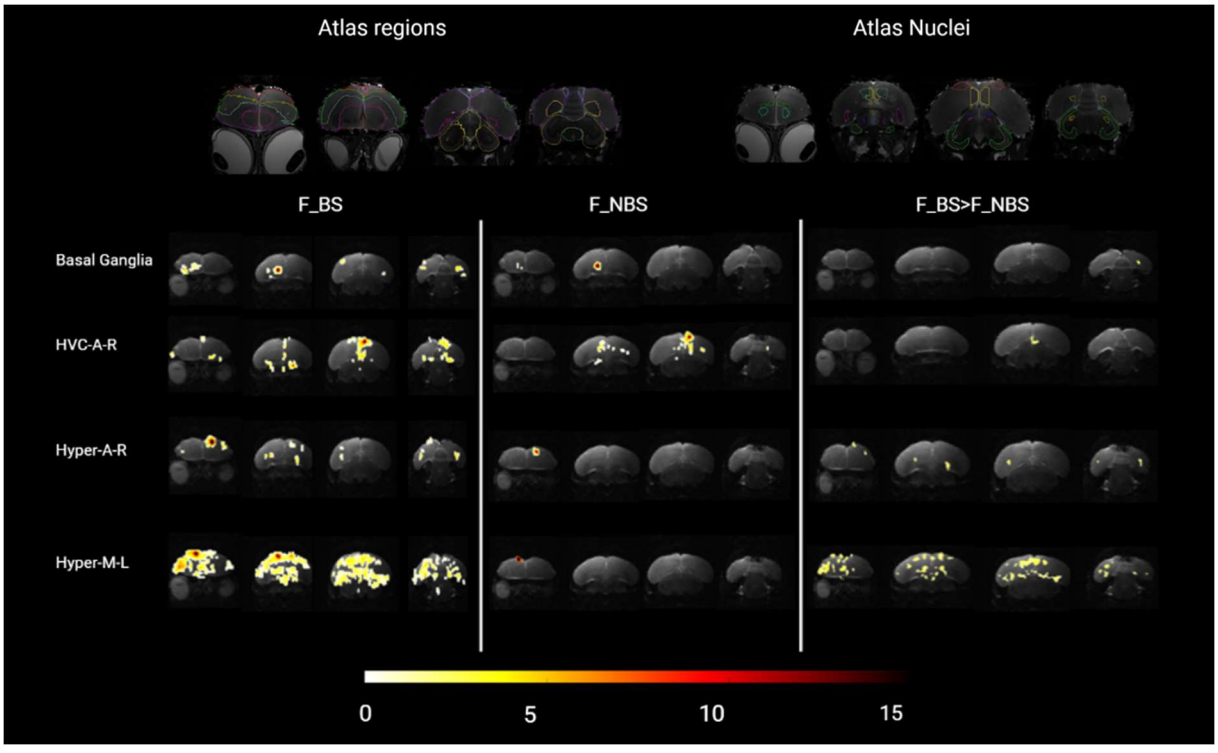

Figure 25: Results of the seed-based analysis for non-GSR data, reveal more connectivity in the breeding season compared to the non-breeding season. The first two columns are the results from the first level group level one-sample T-test seed-based analysis for the females, FDR corrected p<0.05, clustersize (k>10). The last column is the result of the second level two-sample T-test seed-based analysis, FDR corrected p<0.05, clustersize (k>10). The colour bar represents T-values of only positively correlated values, no anti-correlations are shown. The upper row shows renders of the atlas regions from figure 8, the first four pictures show regions, the next four show nuclei.

For the females, the basal ganglia are differently connected with the arcopallial region. HVC-A-R is in the breeding season more connected to parts of the ventricles. In the non-breeding season however, the connection with RA is more significant than in the breeding season. Hyper-A-R is connected to parts of the nidopallium and the basal ganglia. Hyper-M-L is connected to the NCM, NCL-L, parts of the nidopallium and the basal ganglia.

For the males, the same order of statistical tests is used as in the females. The second-level analysis shows again a difference where the connection is higher in the breeding season compared to the non-breeding season.

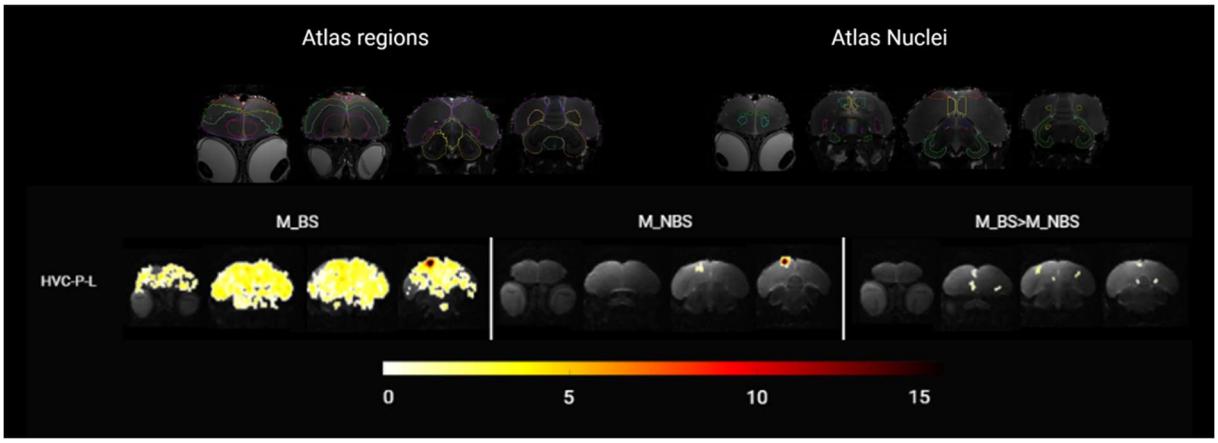

Figure 26: Results of the seed-based analysis for non-GSR data, reveal more connectivity in the breeding season compared to the non-breeding season. The first two columns are the results from the first level group level seed-based analysis for the males, FDR corrected p<0.05, clustersize (k>10). The last column is the result of the second level seed-based analysis, two-sample T-test, FDR corrected p<0.05, clustersize (k>10). The colour bar represents T-values of only positively correlated values, no anti-correlations shown. The upper row shows renders of the atlas regions from figure 8, the first four pictures show regions, the next four show nuclei.

In figure 26, the difference between the two seasons can be seen for the males. A connection of HVC-P-L with RA and Area X is more prominent in the breeding season compared to the non-breeding season. These nuclei are part of the song control system.

6.3.2 Results GSR

For the GSR results the same order is maintained as for the non-GSR results. In the last column the connection in the breeding season is stronger than in the non-breeding season. All the shown results are positive correlations, an analysis for anti-correlations has not been performed.

For the females, there is only a difference in Hyper-M-L over the seasons, the difference is in the region of the seed itself (figure 27).

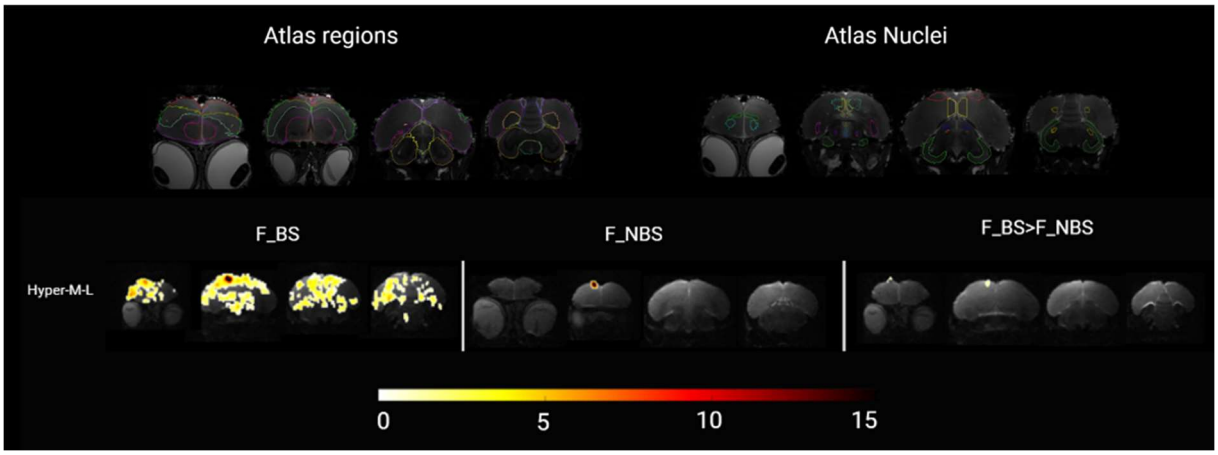

Figure 27: Results of the seed-based analysis for GSR data, reveal more connectivity in the breeding season compared to the non-breeding season. The first two columns are the results from the first level group level seed-based analysis for the females, FDR corrected p<0.05, clustersize(k>10). The last column is the result of the second level seed-based analysis, two-sample T-test, FDR corrected p<0.05, clustersize (k>10). The colour bar represents T-values of only positively correlated values, no anti-correlations shown. The upper row shows renders of the atlas regions from figure 8, the first four pictures show regions, the next four show nuclei.

In the males, figure 28, the second-level analysis reveals again more connections in the breeding season compared to the non-breeding season.

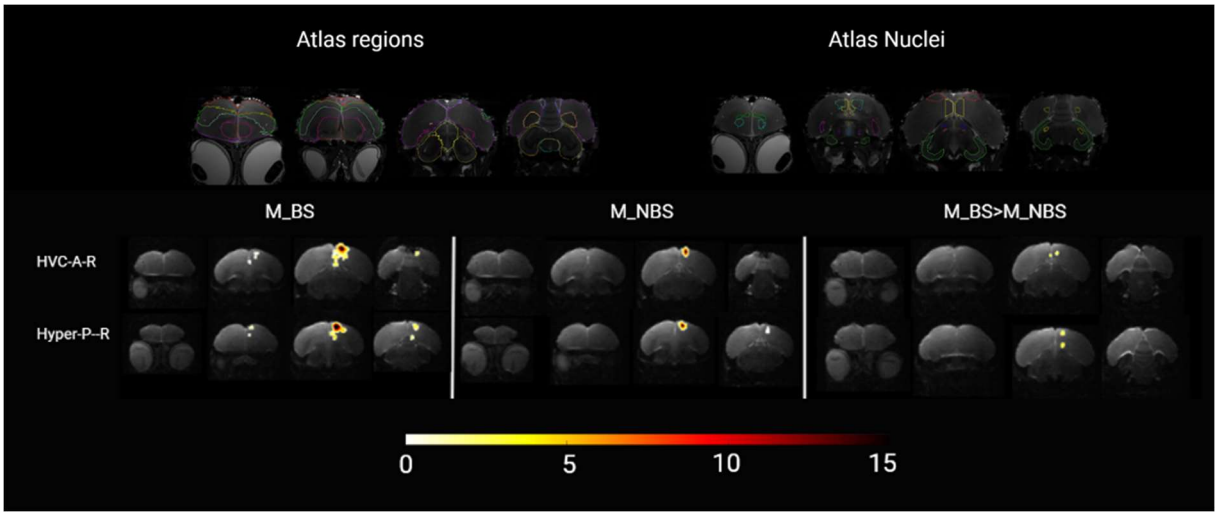

Figure 28: Results of the seed-based analysis for GSR data, reveal more connectivity in the breeding season compared to the non-breeding season. The first two columns are the results from the first level group level seed-based analysis for the males, FDR corrected p<0.05, clustersize (k>10). The last column is the result of the second level seed-based analysis, two-sample T-test, FDR corrected p<0.05, clustersize (k>10). The colour bar represents T-values of only positively correlated values, no anti-correlations shown. The upper row shows renders of the atlas regions from figure 8, the first four pictures show regions, the next four show nuclei.

In figure 28, we can see that for the males there is a stronger connection for HVC-A-R with the NCM and partly field-L and the ventricles. The Hyper-P-R connects differently with CMM-R and part of the basal ganglia.

The same seed appears significantly different in both non-GSR and GSR data, the Hyper-M-L seed in the females. However, in non-GSR data many voxels are different between the seasons. Using GSR corrected data, we find only an extension of the seed which is significantly different in the breeding season compared to the non-breeding season. In general, less differences are found using GSR compared to non-GSR. When we compared the results of the two techniques, FC matrices and seed-based analysis, no overlapping results were found.

7 Discussion

A first aim of this project was to investigate whether rs-fMRI was feasible in starlings. ICA analysis is the preferred method for a data-driven approach for rs-fMRI when there is no prior knowledge about the FC in the species of interest nor a concrete research paradigm to be tested.[87] When we performed ICA analysis for 25 components, we found 25 unique components, that represented specific connectivity maps including either, one or several regions. Further rs-fMRI analysis is possible because we can assess FC in these starlings.

A second aim of this project was to investigate the functional differences between the breeding season and the non-breeding season. When performing a two-sample T-test on the independent components, no significant differences were observed after multiple comparison correction. However, some differences were found when we performed ICA on the groups separate and visually compared which components come out of that analysis. The components of the females in the breeding season contained parts of the visual system while the males in the breeding season have a component for the arcopallium. The arcopallium is known to be involved in motor activity. It also contains RA, which is part of the song control system that is connected to respiratory motor neurons and to muscles of the vocal organs.[88] The involvement of RA in the song control system could be an explanation as to why this component is seen in males and not in females, as males are more proficient singers. Lesions in the visual system, more specifically the entopallium, in pigeons have shown to affect discrimination between two species and between conspecifics.[89,90] This indicates that the entopallium is involved in discrimination between birds, which could be a potential reason why this region comes out of the ICA analysis only for the females. A female starling would need an intact entopallium and potentially a higher functionally activated entopallium to choose a suitable mate during the breeding season. Starlings have a very colourful feathering and an ultraviolet (UV) reflectant plumage, which is not visible to humans as we cannot pick up UV radiation (<400 nm). A study has shown that female starlings are influenced by this UV reflection when choosing a mate for the breeding season. The chosen birds are those with low UV and green reflectance while at the same time high violet and red wavelengths.[91] Most of the components were found in the ICA analysis are unilateral. This could be due to the lateralization in the birdbrain and the fact that there is no corpus callosum, only small commissures.

The FC matrices showed visually a big difference in connectivity. However, the results of the two-sample T-test showed no significant differences upon multiple comparison testing correction (FDR, $p<0.05$). However, since this technique has not been used in this species before, explorative observations are of value, despite the non-significant results.

The comparison between the sexes in the uncorrected, non-GSR matrices leads to few consistent differences between the seasons: NCL-L with Hippocampus, HVC-P-LR with Hippocampus, HVC-A-LR with Hyper-P-L, Hippocampus with Hyper-P-L and Hyper-M-R with Hyper-P-R. The difference in connection with HVC regions, with a higher connectivity in the breeding season than in the non-breeding season, can be explained by the fact that the song control system is bigger in volume in the breeding season and thus the functional connection to the song control nuclei are also expected to be stronger.[43] Most of these regions, except NCL-L, are located at the superior part of the brain. In this part the hyperpallium is located, which comprises the wulst. This is a region known to be part of the visual system and the somatosensory system. This could indicate that there is a difference between seasons for the visual or somatosensory system. The hippocampus is responsible for spatial memory. In the breeding season, this could be more important because of the search for nesting sites and extra food opportunities for the newborn chicks.[92] The connection between the hippocampus and the NCL-L, which is the avian PFC, can be explained by the fact that the PFC accumulates the context of interrelated memories and controls the specificity of memory retrieval. This makes sure that appropriate memories are retrieved within a given context.[93] This difference over the seasons could be attributed to the search for nesting locations and food as well.

One of the possible reasons no significant differences were found using FDR correction could be because there is a large variability in the data. There could be variation due to physiological causes such as size of the bird, age, and testosterone concentration. Not only inevitable physiological variation but also variation when acquiring data is a potential factor. This could be due to the time of day when the scan is recorded, the stress caused by handling the animal or the dosage of anaesthesia. There is no information about the song performance of these birds or the testosterone concentrations at the time of the scans. There is, however, information about the beak colours. Starlings change the colour of their beak in the breeding season, it becomes more yellow while in the non-breeding season it is black. This change is manifested by the concentration of carotenoids and vitamin A in the plasma of the starling[94] and by testosterone.[95] In our dataset, not all beaks were fully yellow yet, which might indicate that not all birds were completely in the breeding season, this could affect the results and cause extra variation in the data. Evidently, another reason for the lack of significant differences upon FDR correction could be because there is no difference between the breeding and the non-breeding season. This would mean that all the differences present in the uncorrected data are false positive results.

In the GSR results, one seasonal FC difference is found using FDR connection. This is the posterior HVC with the anterior hyperpallium, where the FC is stronger in the non-breeding season compared to the breeding season. In the group matrices, this connection is anti-correlated in the breeding season. This part of the hyperpallium matches with the somatosensory wulst. Retinaldehyde dehydrogenase, which plays a critical role in neural development, is expressed similarly in HVC and the hyperpallium apicale, which includes our region. In one research, in zebra finches, it is described to disrupt normal song development when blocked in juveniles. This could indicate that there could be a connection there, although it is not mentioned as such in the literature.[96] If the aforementioned connection is in fact present, there could be an anticorrelation effect between the hyperpallium apicale and the HVC in the breeding season. When comparing the difference matrices for both sexes, no significant similarities were found.

In the seed-based analysis, the differences we found were always when FC was higher in the breeding season than in the non-breeding season. This confirms our hypothesis that the FC will be higher in the breeding season. In non-GSR data for the males, we find an interesting difference in HVC with Area X and RA. These differences have previously been shown structurally in starlings[2,97], our results strengthen previous findings using a different modality. The plasticity in the song control system is thus structurally and functionally present. In male GSR data, this connection is not found, emphasizing the effect of applying GSR. This indicates once more the importance of research toward these modalities and to find out which one is the most scientifically correct.

Pavlova et al. studied the song pattern of female starlings and showed that they sing until half April, which is the middle of the breeding season. After that, they don't sing anymore until October, which is the non-breeding season.[18] When we look at the uncorrected data, we find a difference in connection in HVC-RA where the connection is stronger in the non-breeding season compared to the breeding season (supplementary figure 4). When removing an outlier from the females in the breeding season, the significance for this connection is $p<0.01$. This result could support the findings of Pavlova about the singing behaviour, since the data for the non-breeding season is recorded in October, this coincides with the restart of singing seen in female starlings. The data for the breeding season however is acquired from the end of March until mid-April, which could be a reason as to why there is no significant difference using FDR correction if some females still sing while others do not. For the female data, interpretation is harder than for male data because not every female sings. Only larger females sing across different seasons, indicating that the size of the bird is important.[97] Pavlova also showed that females sing more when occupying a nest box, which were not present in the current study. In this study, males and females were group housed the entire time, another finding from Pavlova et al. was that females sing less when males are present.[18] In our study, males and females were co-housed. These could thus all be confounding factors in our study. No information is known about the singing behaviour or the size of our starlings, this can thus not be used to exclude birds or explain the results.

For the female, non-GSR data four seasonal differences were revealed. Hyper-M-L with NCM, NCL-L, basal ganglia and other parts of the nidopallium. Hyper-M-L is a part of the visual wulst. A connection with the basal ganglia

could indicate some kind of visual learning, while the NCL accumulates the context of the visual memories. The connection with the NCM is then not explained as this is an auditory nucleus. It could indicate that the hyperpallium also reserves a part for auditory processing. HVC-A-R is differently connected with parts of the ventricular zone. It is thought that cell proliferation or the growth of new cells happens in the ventricular zone. In Bengalese finches, they injected [^{3}H]thymidine to measure proliferation in the ventricular zone. They found thymidine labelled cells in HVC, indicating that new cells migrate from the ventricular zone to HVC.[98] This indicates some kind of connection between these regions and can also explain why the connection is stronger in the breeding season, as there is known neuroplasticity in HVC. One difference is between the basal ganglia and the arcopallial region. The arcopallium, which contains RA, is important in motor and sensory projections.[99] The basal ganglia, which contain area X, are also known to be involved in motor control. A seasonal difference in that connection could be explained by the increase in singing behaviour in the breeding season for which more motor control and song learning/processing by the forebrain pathway is necessary. Another difference is Hyper-A-R with parts of the nidopallium and the basal ganglia. Hyper-A-R is part of the somatosensory part of the wulst. It is known that, at least in humans, the basal ganglia receive input from somatosensory areas, which could explain the connection.[100]

In the seed-based analysis GSR data for the males, some differences were found. A difference is found in HVC with the ventricular zone. This difference is explained by the formation of new cells in the HVC in the breeding season as described above. Another difference in connection with HVC is found with NCM and field L, which are parts of the auditory system. It has previously been shown in the canary that there is a connection between field L and HVC.[101,102] A seasonal difference in HVC and NCM has been previously shown.[103] Another difference in the GSR data is Hyper-P-R with CMM-R and basal ganglia. CMM-R is a secondary auditory nucleus, a connection with Hyper-P-R could indicate that this part of the hyperpallium is involved in auditory processing. The basal ganglia are involved in voluntary motor movements and various kinds of learning and cognition, this might indicate that Hyper-P-R is involved in some kind of auditory learning. In the females, a difference is only found in Hyper-M-L, showing an expansion in the seed region. Hyper-M-L is a part of the visual wulst. Female starlings pick a mate based on the UV reflectance, which is processed by the visual system. This could explain why the connection is stronger in the breeding season.

We never observe the same result in both hemispheres for any of the applied modalities. This would suggest that lateralization in starlings extends throughout the entire brain rather than being restricted to the hippocampus.

More analysis can be done on this data to gain more knowledge about the FC in starlings. Future research opportunities include: performing a seed-based analysis with other biologically relevant seeds for example from the visual pathway: entopallium or nucleus rotundus. The primary auditory nucleus Field L or RA as this is part of the song control system. This could give us extra information about the differences between the seasons in other parts of the brain. We could also look at the group-level analysis to unravel which networks are present that aren't necessarily different between seasons. In humans and in rodents, some analogous networks are known such as the default mode (like) network (DM(L)N) and the lateral cortical network (LCN, rodents), which is associated with the task-positive network in humans. It is possible that these networks are present in birdbrains as well, however there are large pallial regions in the avian brain for which the function is unknown, this complicates the identification of larger networks such as for example the DMLN. Another future step could be, reperforming the seed-based analysis for the anti-correlation in the birds. This could give additional information about some regions in the starling brain and how it influences other networks.

If this study were to be redone, the scans could be taken on more different time points, to evaluate not only the differences between breeding and non-breeding season, but also to look at the difference between photo-sensitive, photo-refractory (non-breeding season) and the photo-stimulated period (breeding season). This is particularly important for the females since they sing on different moments than the males, and are seen to stop singing when males are induced in the social group[18], although this is not always the case. Before scanning in the breeding season, it might be of value to measure testosterone concentration and look whether the beak is

completely yellow to ensure that the birds are fully in the breeding season to enable a convincing comparison between the different time periods. For the photo-refractory period, it could be useful to look whether the birds are molting, loosing feathers as this period can be marked by that. In the photo-sensitive period, their feathers are normal again and their beak is black. Apart from different scanning times, it would also be important to record the singing to be able to correlate it to the rs-fMRI results. This is again, more important for the female starlings, since not all of them sing (as much) even though they are capable of it.

Now that we confirmed that rs-fMRI is a valuable technique in starlings, we could try using dynamic rs-fMRI to investigate changes of the networks over time. It could give insights about the dynamics of neural activity and could be used to investigate pathology. One dynamic rs-fMRI technique is called co-activation patterns (CAP), they represent transient brain states. When fMRI time frames of a given region of interest cross a specific percentile threshold, they are clustered to identify different CAP's. It can distinguish healthy from diseased animals, and they can potentially be a good biomarker for disease. It could also provide more insight in the seasonal differences in the starlings.[104] Another dynamic rs-fMRI technique is quasi periodic patterns (QPP). It searches recurring consecutive sequences of BOLD volumes called spatiotemporal patterns. This could give insights in the temporal evolution of the resting-state networks.[105]

8 Conclusion

In conclusion, rs-fMRI is a technique that can be used to study networks and certainly differences in networks in this new species, the European starling. We can also conclude that there are more functional connections in the breeding season compared to the non-breeding season, both with and without GSR. To establish which modality is best, more research is needed and cannot be concluded out of our results.

The connections previously found to change structurally in the song control system, the HVC-RA tract, we find in rs-fMRI data as well. This shows that this connection truly changes structurally and functionally between seasons, certainly for the males.

More research is needed to fill in the gaps for bird rs-fMRI in general as not much is known about networks in the songbird brain besides the auditory, visual and song control network. Our project is a start for unravelling potential networks in the starling brain and emphasizes the existence of seasonal functional differences.

9 References

1 Theofanopoulou, C., Boeckx, C. & Jarvis, E. D. A hypothesis on a role of oxytocin in the social mechanisms of speech and vocal learning. *Proc Biol Sci* **284**, doi:10.1098/rspb.2017.0988 (2017).

2 De Groof, G. & Van der Linden, A. Love songs, bird brains and diffusion tensor imaging. *NMR Biomed* **23**, 873-883, doi:10.1002/nbm.1551 (2010).

3 Orije, J. & Van der Linden, A. A brain for all seasons: An in vivo MRI perspective on songbirds. *J Exp Zool A Ecol Integr Physiol* **337**, 967-984, doi:10.1002/jez.2650 (2022).

4 L, L. L. Birdsong and Human Speech and Language: What the Zebra Finch Uses, Loses, and Regains. (2012).

5 Panaitof, S. C. A songbird animal model for dissecting the genetic bases of autism spectrum disorder. *Dis Markers* **33**, 241-249, doi:10.3233/DMA-2012-0918 (2012).

6 Layden, E. A., Schertz, K. E., London, S. E. & Berman, M. G. Interhemispheric functional connectivity in the zebra finch brain, absent the corpus callosum in normal ontogeny. *Neuroimage* **195**, 113-127, doi:10.1016/j.neuroimage.2019.03.064 (2019).

7 Kubikova, L. & Kostal, L. Dopaminergic system in birdsong learning and maintenance. *J Chem Neuroanat* **39**, 112-123, doi:10.1016/j.jchemneu.2009.10.004 (2010).

8 Moorman, S. *et al.* Human-like brain hemispheric dominance in birdsong learning. *Proc Natl Acad Sci U S A* **109**, 12782-12787, doi:10.1073/pnas.1207207109 (2012).

9 Stinnett, T. J., Reddy, V. & Zabel, M. K. in *StatPearls* (2022).

10 Binder, J. R. Current Controversies on Wernicke's Area and its Role in Language. *Curr Neurol Neurosci Rep* **17**, 58, doi:10.1007/s11910-017-0764-8 (2017).

11 Sherman, S. M. Thalamic relay functions. *Prog Brain Res* **134**, 51-69, doi:10.1016/s0079-6123(01)34005-0 (2001).

12 Jarvis, E. D. Learned birdsong and the neurobiology of human language. *Ann N Y Acad Sci* **1016**, 749-777, doi:10.1196/annals.1298.038 (2004).

13 Pinaud, R. & Terleph, T. A. A songbird forebrain area potentially involved in auditory discrimination and memory formation. *J Biosci* **33**, 145-155, doi:10.1007/s12038-008-0030-y (2008).

14 Szaflarski, J. P. *et al.* Language lateralization in left-handed and ambidextrous people: fMRI data. *Neurology* **59**, 238-244, doi:10.1212/wnl.59.2.238 (2002).

15 Hamaide, J. *et al.* In vivo assessment of the neural substrate linked with vocal imitation accuracy. *Elife* **9**, doi:10.7554/eLife.49941 (2020).

16 Jonckers, E., Gunturkun, O., De Groof, G., Van der Linden, A. & Bingman, V. P. Network structure of functional hippocampal lateralization in birds. *Hippocampus* **25**, 1418-1428, doi:10.1002/hipo.22462 (2015).

17 Riters, L. V., Eens, M., Pinxten, R. & Ball, G. F. Seasonal changes in the densities of alpha(2) noradrenergic receptors are inversely related to changes in testosterone and the volumes of song control nuclei in male European starlings. *J Comp Neurol* **444**, 63-74, doi:10.1002/cne.10131 (2002).

18 Pavlova, D. Z., Pinxten, R. & Eens, M. Seasonal singing patterns and individual consistency in song activity in female European starlings (Sturnus vulgaris). *Behaviour* **144**, 663-680, doi:Doi 10.1163/156853907781347835 (2007).

19 Pavlova, D., Pinxten, R. & Eens, M. Female song in European Starlings: Sex differences, complexity, and composition. *Condor* **107**, 559-569, doi:Doi 10.1650/0010-5422(2005)107[0559:Fsiess]2.0.Co;2 (2005).

20 Chaiken, M. L., Böhner Jörg. SONG LEARNING AFTER ISOLATION IN THE OPENENDED LEARNER THE EUROPEAN STARLING:

DISSOCIATION OF IMITATION AND SYNTACTIC

DEVELOPMENT. (2007).

21 Lehongre, K., P. Lenouvel, T. Draganoiu, C. Del Negro. Long-term effect of isolation rearing conditions on songs of an 'open-ended' song learner species, the Canary. (2006).

22 Williams, H. Birdsong and singing behavior. *Ann N Y Acad Sci* **1016**, 1-30, doi:10.1196/annals.1298.029 (2004).

23 Williams, H. Birdsong and singing behavior. *Ann Ny Acad Sci* **1016**, 1-30, doi:10.1196/annals.1298.029 (2004).

24 Nottebohm, F., Nottebohm, M. E. & Crane, L. Developmental and seasonal changes in canary song and their relation to changes in the anatomy of song-control nuclei. *Behav Neural Biol* **46**, 445-471, doi:10.1016/s0163-1047(86)90485-1 (1986).
25 Eens, M., Pinxten, R. & Verheyen, R. F. Song Learning in Captive European Starlings, Sturnus-Vulgaris. *Animal Behaviour* **44**, 1131-1143, doi:Doi 10.1016/S0003-3472(05)80325-2 (1992).
26 Hindmarsh, A. M. Vocal Mimicry in Starlings. *Behaviour* **90**, 302-324, doi:Doi 10.1163/156853984x00182 (1984).
27 George, I. & Cousillas, H. How social experience shapes song representation in the brain of starlings. *J Physiol Paris* **107**, 170-177, doi:10.1016/j.jphysparis.2012.12.002 (2013).
28 Poirier, C. *et al.* Direct social contacts override auditory information in the song-learning process in starlings (Sturnus vulgaris). *J Comp Psychol* **118**, 179-193, doi:10.1037/0735-7036.118.2.179 (2004).
29 Nicholls, T. J., Goldsmith, A. R. & Dawson, A. Photorefractoriness in birds and comparison with mammals. *Physiol Rev* **68**, 133-176, doi:10.1152/physrev.1988.68.1.133 (1988).
30 Gwinner, E. Circannual rhythms in birds. *Curr Opin Neurobiol* **13**, 770-778, doi:10.1016/j.conb.2003.10.010 (2003).
31 Magee, J. C. & Grienberger, C. Synaptic Plasticity Forms and Functions. *Annu Rev Neurosci* **43**, 95-117, doi:10.1146/annurev-neuro-090919-022842 (2020).
32 Patton, M. H., Blundon, J. A. & Zakharenko, S. S. Rejuvenation of plasticity in the brain: opening the critical period. *Curr Opin Neurobiol* **54**, 83-89, doi:10.1016/j.conb.2018.09.003 (2019).
33 Cisneros-Franco, J. M., Voss, P., Thomas, M. E. & de Villers-Sidani, E. Critical periods of brain development. *Handb Clin Neurol* **173**, 75-88, doi:10.1016/B978-0-444-64150-2.00009-5 (2020).
34 Knudsen, E. I. Sensitive periods in the development of the brain and behavior. *J Cogn Neurosci* **16**, 1412-1425, doi:10.1162/0898929042304796 (2004).
35 Zhou, Q., Tao, H. W. & Poo, M. M. Reversal and stabilization of synaptic modifications in a developing visual system. *Science* **300**, 1953-1957, doi:10.1126/science.1082212 (2003).
36 Friedmann, N. & Rusou, D. Critical period for first language: the crucial role of language input during the first year of life. *Curr Opin Neurobiol* **35**, 27-34, doi:10.1016/j.conb.2015.06.003 (2015).
37 Fitzpatrick, E. Neurocognitive development in congenitally deaf children. *Handb Clin Neurol* **129**, 335-356, doi:10.1016/B978-0-444-62630-1.00019-6 (2015).
38 Kral, A. & Sharma, A. Developmental neuroplasticity after cochlear implantation. *Trends in Neurosciences* **35**, 111-122, doi:10.1016/j.tins.2011.09.004 (2012).
39 Holmes, J. M. & Levi, D. M. Treatment of amblyopia as a function of age. *Vis Neurosci* **35**, E015, doi:10.1017/S0952523817000220 (2018).
40 Ismail, F. Y., Fatemi, A. & Johnston, M. V. Cerebral plasticity: Windows of opportunity in the developing brain. *Eur J Paediatr Neurol* **21**, 23-48, doi:10.1016/j.ejpn.2016.07.007 (2017).
41 Roder, B. & Kekunnaya, R. Visual experience dependent plasticity in humans. *Curr Opin Neurobiol* **67**, 155-162, doi:10.1016/j.conb.2020.11.011 (2021).
42 Hamaide, J., De Groof, G. & Van der Linden, A. Neuroplasticity and MRI: A perfect match. *Neuroimage* **131**, 13-28, doi:10.1016/j.neuroimage.2015.08.005 (2016).
43 De Groof, G. *et al.* Structural changes between seasons in the songbird auditory forebrain. *J Neurosci* **29**, 13557-13565, doi:10.1523/JNEUROSCI.1788-09.2009 (2009).
44 Villemagne, V. L. *et al.* Molecular Imaging Approaches in Dementia. *Radiology* **298**, 517-530, doi:10.1148/radiol.2020200028 (2021).
45 Dorbala, S. *et al.* Single Photon Emission Computed Tomography (SPECT) Myocardial Perfusion Imaging Guidelines: Instrumentation, Acquisition, Processing, and Interpretation. *J Nucl Cardiol* **25**, 1784-1846, doi:10.1007/s12350-018-1283-y (2018).
46 Flohr, T. *et al.* Photon-counting CT review. *Phys Med* **79**, 126-136, doi:10.1016/j.ejmp.2020.10.030 (2020).
47 Fonti, R., Conson, M. & Del Vecchio, S. PET/CT in radiation oncology. *Semin Oncol* **46**, 202-209, doi:10.1053/j.seminoncol.2019.07.001 (2019).
48 Zeng, D. *et al.* Basis and current state of computed tomography perfusion imaging: a review. *Phys Med Biol* **67**, doi:10.1088/1361-6560/ac8717 (2022).
49 Yousaf, T., Dervenoulas, G. & Politis, M. Advances in MRI Methodology. *Int Rev Neurobiol* **141**, 31-76, doi:10.1016/bs.irn.2018.08.008 (2018).
50 Grover, V. P. *et al.* Magnetic Resonance Imaging: Principles and Techniques: Lessons for Clinicians. *J Clin Exp Hepatol* **5**, 246-255, doi:10.1016/j.jceh.2015.08.001 (2015).

51 Weiger, M. & Pruessmann, K. P. Short-T(2) MRI: Principles and recent advances. *Prog Nucl Magn Reson Spectrosc* **114-115**, 237-270, doi:10.1016/j.pnmrs.2019.07.001 (2019).
52 Gauthier, C. J. & Fan, A. P. BOLD signal physiology: Models and applications. *Neuroimage* **187**, 116-127, doi:10.1016/j.neuroimage.2018.03.018 (2019).
53 Logothetis, N. K. What we can do and what we cannot do with fMRI. *Nature* **453**, 869-878, doi:10.1038/nature06976 (2008).
54 Rangaprakash, D., Tadayonnejad, R., Deshpande, G., O'Neill, J. & Feusner, J. D. FMRI hemodynamic response function (HRF) as a novel marker of brain function: applications for understanding obsessive-compulsive disorder pathology and treatment response. *Brain Imaging Behav* **15**, 1622-1640, doi:10.1007/s11682-020-00358-8 (2021).
55 Rangaprakash, D., Wu, G. R., Marinazzo, D., Hu, X. & Deshpande, G. Hemodynamic response function (HRF) variability confounds rng-state fMRI functional connectivity. *Magn Reson Med* **80**, 1697-1713, doi:10.1002/mrm.27146 (2018).
56 Jackson, G. D., Badawy, R. & Gotman, J. Functional magnetic resonance imaging: focus localization. *Handb Clin Neurol* **107**, 369-385, doi:10.1016/B978-0-444-52898-8.00023-9 (2012).
57 Dupuy, S. L. *et al.* MRI detection of hypointense brain lesions in patients with multiple sclerosis: T1 spin-echo vs. gradient-echo. *Eur J Radiol* **84**, 1564-1568, doi:10.1016/j.ejrad.2015.05.004 (2015).
58 Poustchi-Amin, M., Mirowitz, S. A., Brown, J. J., McKinstry, R. C. & Li, T. Principles and applications of echo-planar imaging: a review for the general radiologist. *Radiographics* **21**, 767-779, doi:10.1148/radiographics.21.3.g01ma23767 (2001).
59 Behroozi, M. *et al.* In vivo measurement of T(1) and T(2) relaxation times in awake pigeon and rat brains at 7T. *Magn Reson Med* **79**, 1090-1100, doi:10.1002/mrm.26722 (2018).
60 De Groof, G. *et al.* Functional MRI and functional connectivity of the visual system of awake pigeons. *Behav Brain Res* **239**, 43-50, doi:10.1016/j.bbr.2012.10.044 (2013).
61 Van Ruijssevelt, L., Hamaide, J., Van Gurp, M. T., Verhoye, M. & Van der Linden, A. Auditory evoked BOLD responses in awake compared to lightly anaesthetized zebra finches. *Sci Rep* **7**, 13563, doi:10.1038/s41598-017-13014-x (2017).
62 Steiner, A. R., Rousseau-Blass, F., Schroeter, A., Hartnack, S. & Bettschart-Wolfensberger, R. Systematic Review: Anesthetic Protocols and Management as Confounders in Rodent Blood Oxygen Level Dependent Functional Magnetic Resonance Imaging (BOLD fMRI)-Part B: Effects of Anesthetic Agents, Doses and Timing. *Animals (Basel)* **11**, doi:10.3390/ani11010199 (2021).
63 Kelly, C. & Castellanos, F. X. Strengthening connections: functional connectivity and brain plasticity. *Neuropsychol Rev* **24**, 63-76, doi:10.1007/s11065-014-9252-y (2014).
64 Fox, M. D. & Greicius, M. Clinical applications of resting state functional connectivity. *Front Syst Neurosci* **4**, 19, doi:10.3389/fnsys.2010.00019 (2010).
65 Raichle, M. E. & Mintun, M. A. Brain work and brain imaging. *Annu Rev Neurosci* **29**, 449-476, doi:10.1146/annurev.neuro.29.051605.112819 (2006).
66 Raichle, M. E. Neuroscience. The brain's dark energy. *Science* **314**, 1249-1250 (2006).
67 Jahanian, H. *et al.* Advantages of short repetition time resting-state functional MRI enabled by simultaneous multi-slice imaging. *J Neurosci Methods* **311**, 122-132, doi:10.1016/j.jneumeth.2018.09.033 (2019).
68 Grandjean, J. *et al.* Psilocybin exerts distinct effects on resting state networks associated with serotonin and dopamine in mice. *Neuroimage* **225**, doi:ARTN 117456

10.1016/j.neuroimage.2020.117456 (2021).
69 Vasilkovska, T. *et al.* Resting-state fMRI reveals longitudinal alterations in brain network connectivity in the zQ175DN mouse model of Huntington's disease. *Neurobiol Dis* **181**, 106095, doi:10.1016/j.nbd.2023.106095 (2023).
70 Liang, Z., Liu, X. & Zhang, N. Dynamic resting state functional connectivity in awake and anesthetized rodents. *Neuroimage* **104**, 89-99, doi:10.1016/j.neuroimage.2014.10.013 (2015).
71 Behroozi, M., Strockens, F., Helluy, X., Stacho, M. & Gunturkun, O. Functional Connectivity Pattern of the Internal Hippocampal Network in Awake Pigeons: A Resting-State fMRI Study. *Brain Behav Evol* **90**, 62-72, doi:10.1159/000475591 (2017).
72 Baggio, H. C., Segura, B. & Junque, C. Resting-state functional brain networks in Parkinson's disease. *CNS Neurosci Ther* **21**, 793-801, doi:10.1111/cns.12417 (2015).
73 Xing, C. *et al.* Abnormal Static and Dynamic Functional Network Connectivity in Patients With Presbycusis. *Front Aging Neurosci* **13**, 774901, doi:10.3389/fnagi.2021.774901 (2021).

74 Stacho, M. *et al.* A cortex-like canonical circuit in the avian forebrain. *Science* **369**, doi:10.1126/science.abc5534 (2020).
75 Marzluff, J. M., Miyaoka, R., Minoshima, S. & Cross, D. J. Brain imaging reveals neuronal circuitry underlying the crow's perception of human faces. *Proc Natl Acad Sci U S A* **109**, 15912-15917, doi:10.1073/pnas.1206109109 (2012).
76 Gunturkun, O. & Bugnyar, T. Cognition without Cortex. *Trends Cogn Sci* **20**, 291-303, doi:10.1016/j.tics.2016.02.001 (2016).
77 Layden, E. A., Li, H. B., Schertz, K. E., Berman, M. G. & London, S. E. Experience selectively alters functional connectivity within a neural network to predict learned behavior in juvenile songbirds. *Neuroimage* **222**, doi:ARTN 117218

10.1016/j.neuroimage.2020.117218 (2020).
78 De Groof, G. *et al.* Functional MRI and functional connectivity of the visual system of awake pigeons. *Behavioural Brain Research* **239**, 43-50, doi:10.1016/j.bbr.2012.10.044 (2013).
79 Orije, J. *et al.* In vivo online monitoring of testosterone-induced neuroplasticity in a female songbird. *Horm Behav* **118**, 104639, doi:10.1016/j.yhbeh.2019.104639 (2020).
80 Tong, Y., Hocke, L. M. & Frederick, B. B. Low Frequency Systemic Hemodynamic "Noise" in Resting State BOLD fMRI: Characteristics, Causes, Implications, Mitigation Strategies, and Applications. *Front Neurosci* **13**, 787, doi:10.3389/fnins.2019.00787 (2019).
81 Wu, Z., Huang, N. E., Long, S. R. & Peng, C. K. On the trend, detrending, and variability of nonlinear and nonstationary time series. *Proc Natl Acad Sci U S A* **104**, 14889-14894, doi:10.1073/pnas.0701020104 (2007).
82 Lee, D., Jang, C. & Park, H. J. Multivariate detrending of fMRI signal drifts for real-time multiclass pattern classification. *Neuroimage* **108**, 203-213, doi:10.1016/j.neuroimage.2014.12.062 (2015).
83 Li, J. *et al.* Global signal regression strengthens association between resting-state functional connectivity and behavior. *Neuroimage* **196**, 126-141, doi:10.1016/j.neuroimage.2019.04.016 (2019).
84 Chang, C. *et al.* Tracking brain arousal fluctuations with fMRI. *Proc Natl Acad Sci U S A* **113**, 4518-4523, doi:10.1073/pnas.1520613113 (2016).
85 Calhoun, V. D., Adali, T., Pearlson, G. D. & Pekar, J. J. A method for making group inferences from functional MRI data using independent component analysis. *Hum Brain Mapp* **14**, 140-151, doi:10.1002/hbm.1048 (2001).
86 De Groof, G. *et al.* A three-dimensional digital atlas of the starling brain. *Brain Struct Funct* **221**, 1899-1909, doi:10.1007/s00429-015-1011-1 (2016).
87 Zhao, W. *et al.* Consistency of independent component analysis for FMRI. *J Neurosci Methods* **351**, 109013, doi:10.1016/j.jneumeth.2020.109013 (2021).
88 Jarvis, E. D. *et al.* Avian brains and a new understanding of vertebrate brain evolution. *Nature Reviews Neuroscience* **6**, 151-159, doi:10.1038/nrn1606 (2005).
89 Watanabe, S. Effects of ectostriatal lesions on discriminations of conspecific, species and familiar objects in pigeons. *Behav Brain Res* **81**, 183-188, doi:10.1016/s0166-4328(96)89079-6 (1996).
90 Watanabe, S. Effect of lesions in the ectostriatum and Wulst on species and individual discrimination in pigeons. *Behav Brain Res* **49**, 197-203, doi:10.1016/s0166-4328(05)80165-2 (1992).
91 Bennett, A. T., Cuthill, I. C., Partridge, J. C. & Lunau, K. Ultraviolet plumage colors predict mate preferences in starlings. *Proc Natl Acad Sci U S A* **94**, 8618-8621, doi:10.1073/pnas.94.16.8618 (1997).
92 Oberlander, J. G., Schlinger, B. A., Clayton, N. S. & Saldanha, C. J. Neural aromatization accelerates the acquisition of spatial memory via an influence on the songbird hippocampus. *Horm Behav* **45**, 250-258, doi:10.1016/j.yhbeh.2003.12.003 (2004).
93 Preston, A. R. & Eichenbaum, H. Interplay of hippocampus and prefrontal cortex in memory. *Curr Biol* **23**, R764-773, doi:10.1016/j.cub.2013.05.041 (2013).
94 Navarro, C., Perez-Contreras, T., Aviles, J. M., Mcgraw, K. J. & Soler, J. J. Beak colour reflects circulating carotenoid and vitamin A levels in spotless starlings (Sturnus unicolor). *Behavioral Ecology and Sociobiology* **64**, 1057-1067, doi:10.1007/s00265-010-0920-5 (2010).
95 Gregory F. Ball, J. C. W. Changes in Plasma Levels of Luteinizing Hormone and Sex Steroid Hormones in Relation to Multiple-Broodedness and Nest-Site Density in Male Starlings. *Physiological Zoology* **60**.
96 Kim, Y. H. & Arnold, A. P. Distribution and onset of retinaldehyde dehydrogenase (zRalDH) expression in zebra finch brain: lack of sex difference in HVC and RA at early posthatch ages. *J Neurobiol* **65**, 260-268, doi:10.1002/neu.20192 (2005).

97 Orije, J. *et al.* Uncovering a 'sensitive window' of multisensory and motor neuroplasticity in the cerebrum and cerebellum of male and female starlings. *Elife* **10**, doi:10.7554/eLife.66777 (2021).
98 Zeng, S. J., Song, K., Xu, N., Zhang, X. W. & Zuo, M. X. Sex difference in cellular proliferation within the telencephalic ventricle zone of Bengalese finch. *Neurosci Res* **58**, 207-214, doi:10.1016/j.neures.2007.02.001 (2007).
99 Mello, C. V., Kaser, T., Buckner, A. A., Wirthlin, M. & Lovell, P. V. Molecular architecture of the zebra finch arcopallium. *J Comp Neurol* **527**, 2512-2556, doi:10.1002/cne.24688 (2019).
100 Beudel, M., Macerollo, A., Brown, M. J. N. & Chen, R. Editorial: The Role of the Basal Ganglia in Somatosensory-Motor Interactions: Evidence From Neurophysiology and Behavior. *Front Hum Neurosci* **13**, 451, doi:10.3389/fnhum.2019.00451 (2019).
101 Kelley, D. B. & Nottebohm, F. Projections of a telencephalic auditory nucleus-field L-in the canary. *J Comp Neurol* **183**, 455-469, doi:10.1002/cne.901830302 (1979).
102 Zaretsky, M. D. A new auditory area of the songbird forebrain: a connection between auditory and song control centers. *Exp Brain Res* **32**, 267-273, doi:10.1007/BF00239731 (1978).
103 De Groof, G., Poirier, C., George, I., Hausberger, M. & Van der Linden, A. Functional changes between seasons in the male songbird auditory forebrain. *Front Behav Neurosci* **7**, 196, doi:10.3389/fnbeh.2013.00196 (2013).
104 Adhikari, M. H., Belloy, M. E., Van der Linden, A., Keliris, G. A. & Verhoye, M. Resting-State Co-activation Patterns as Promising Candidates for Prediction of Alzheimer's Disease in Aged Mice. *Front Neural Circuits* **14**, 612529, doi:10.3389/fncir.2020.612529 (2020).
105 Belloy, M. E. *et al.* Dynamic resting state fMRI analysis in mice reveals a set of Quasi-Periodic Patterns and illustrates their relationship with the global signal. *Neuroimage* **180**, 463-484, doi:10.1016/j.neuroimage.2018.01.075 (2018).

10 Acknowledgements

First, I would like to express my gratitude to my promotor Prof. Dr. Marleen Verhoye to give me the opportunity to do my internship in the Bio-imaging lab. After doing my bachelor internship there, I was truly fascinated by the many opportunities of MRI and therefore extra grateful that I could start my master internship here as well. I would also like to thank Prof. Dr. Annemie van der linden and Dr. Jasmien Orije for sharing their expertise on starlings and their brains. A last supervisor I'd like to thank is (almost Dr. 😊) Tamara Vasilkovska for sharing her expertise on rs-fMRI and MATLAB codes. All of you contributed to the creation of my thesis and to my growth as a researcher and as a person by giving me very valuable feedback and guidance.

I would also like to thank Christien Bowman for trusting me with the further practical execution of his project. It has taught me a lot in terms of science but also project management, animal care, flexibility and most importantly it has shown me what I want to do in my future career.

A special credit goes to Ignace Van Spilbeeck for always helping me with my MATLAB problems, no matter how ridiculous they were. I truly admire your coding skills and there is a lot more to learn from you. The lab should be really grateful to have you to help with their problems. Johan Van Audekerke, a special thanks goes to you for always helping me with any practical problems and for always making me laugh.

At last, I would like to thank some other members of the Bio-imaging lab. Judith Van Rooij for always jumping to help me with my emergency situations 😊, Nick Vidas-Gusic, Joëlle Van Rijswijk, Sam De Waegenaere and Leonardo Ricciardi to help me when I needed it. I had an amazing time in the lab performing research, encountering and solving problems and making conversation with all of you!

11 Supplementary material

11.1 Independent components

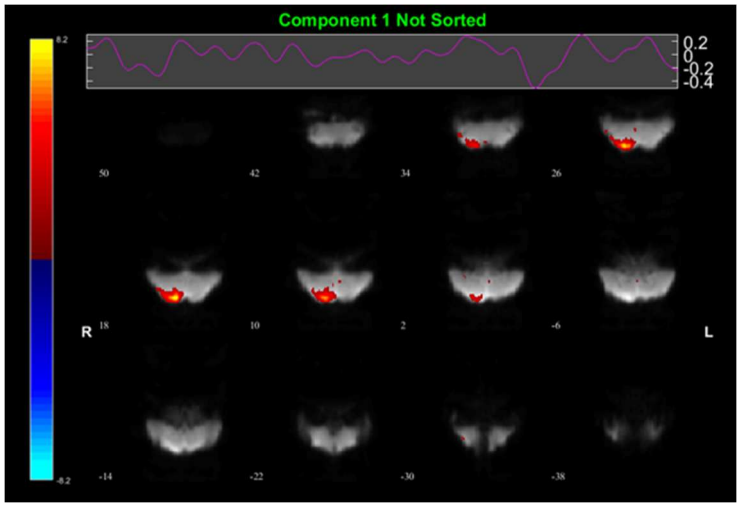

Component 1: Hyper-P-L

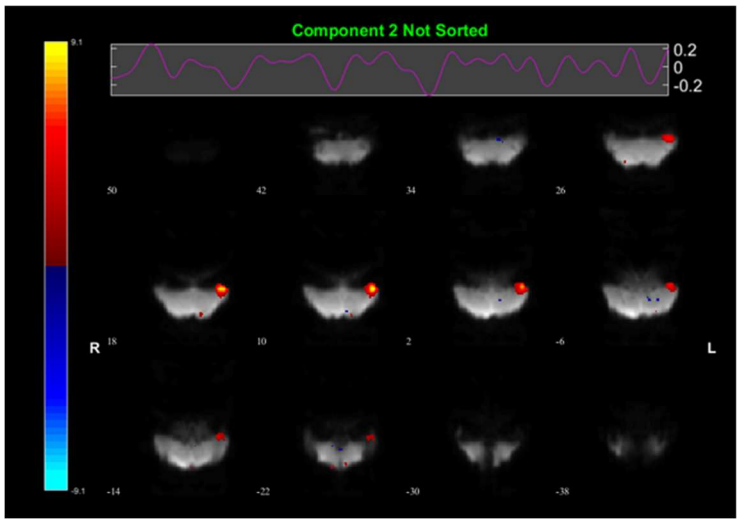

Component 2: Nido-M-I-R

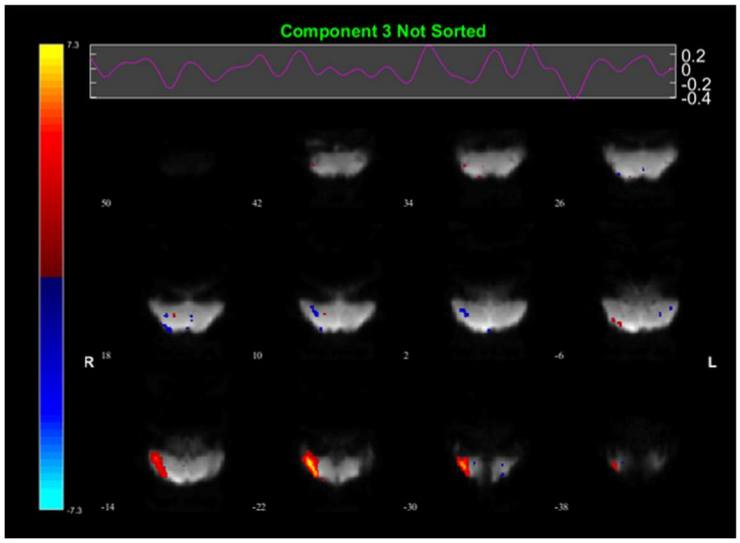

Component 3: Nido-P-int-L

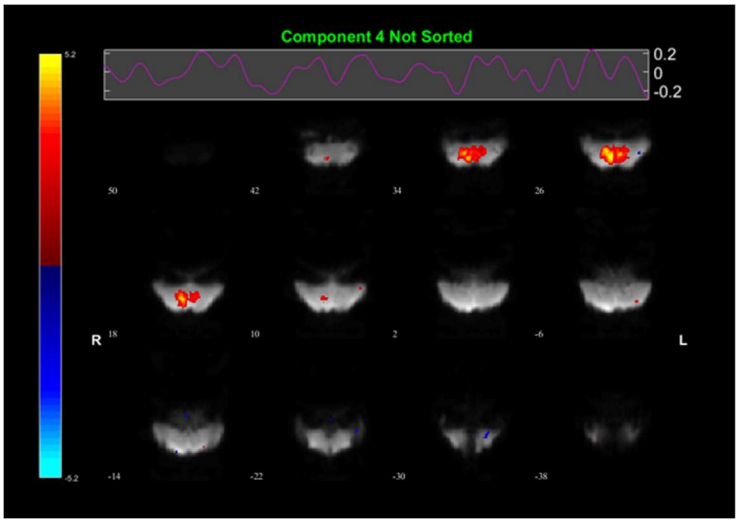

Component 4: Area X

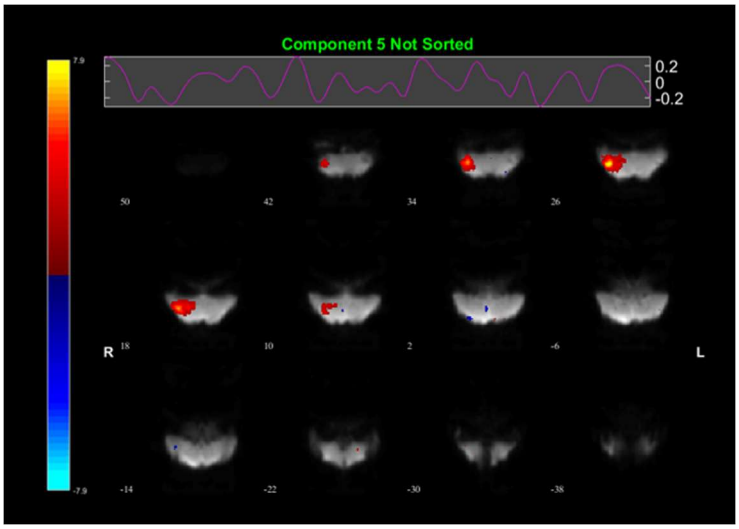

Component 5: Nido-A-int-L

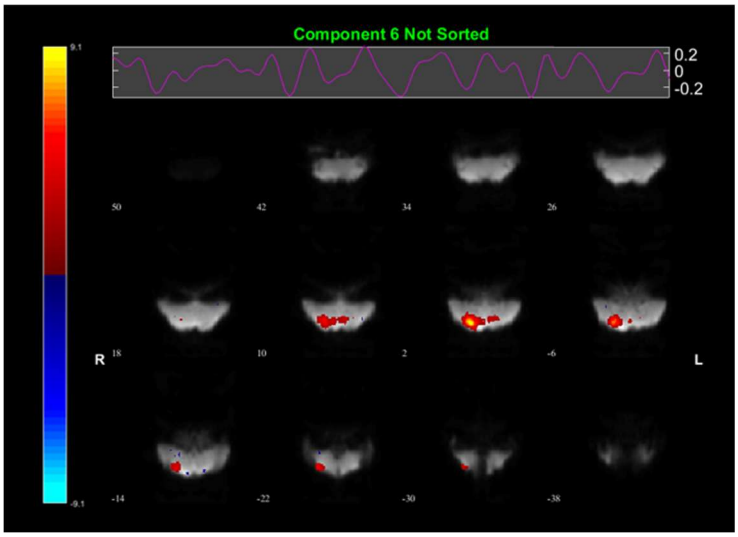

Component 6: Nido-M-S-L

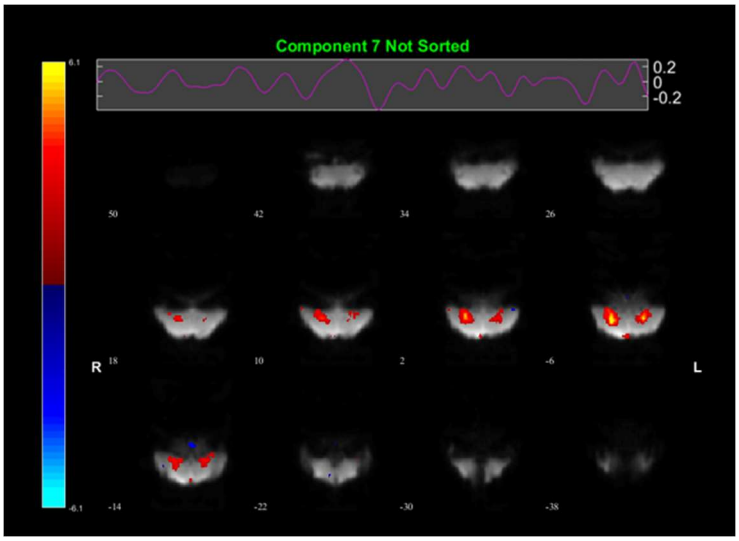

Component 7: Basal ganglia

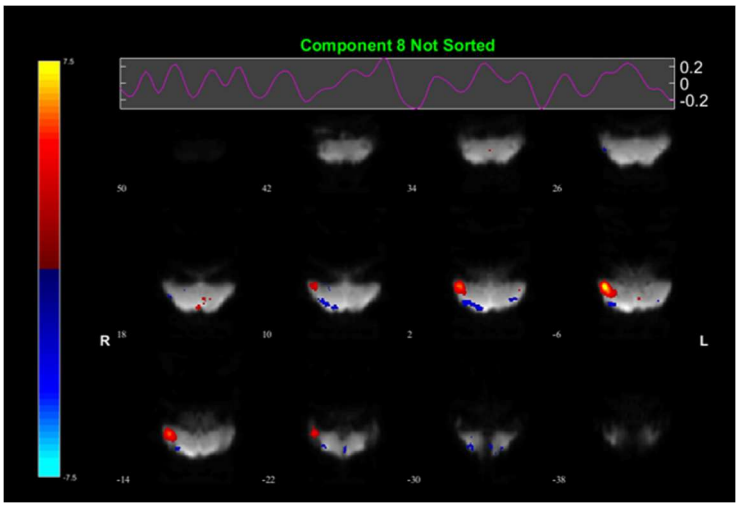

Component 8: Nido-PM-I-L

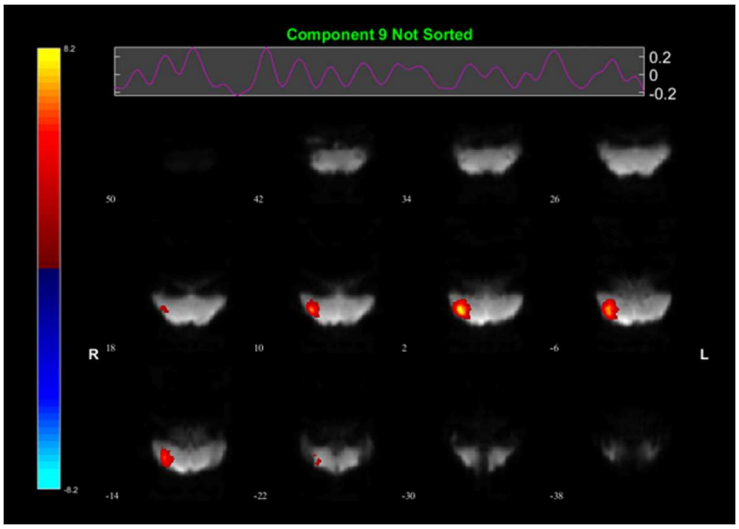

Component 9: Nido-M-int-L

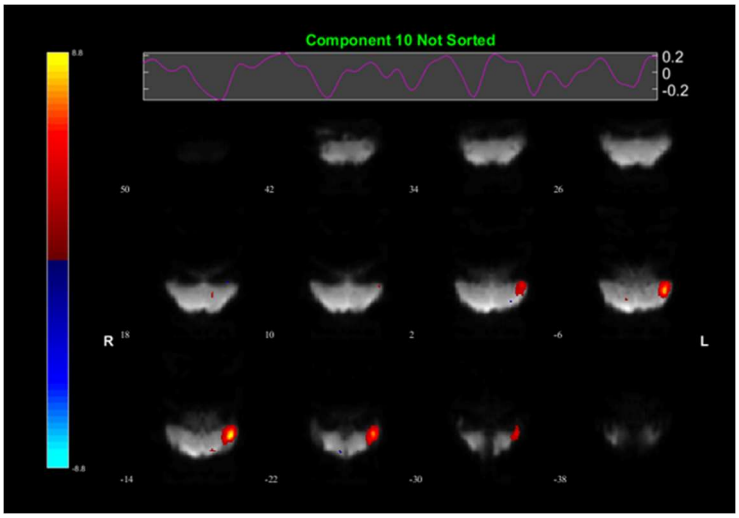

Component 10: Nido-PM-I-R

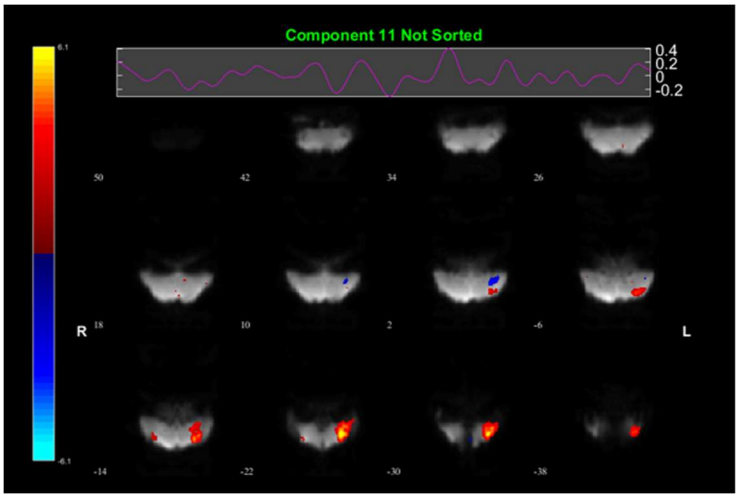

Component 11: Nido-P-int-R

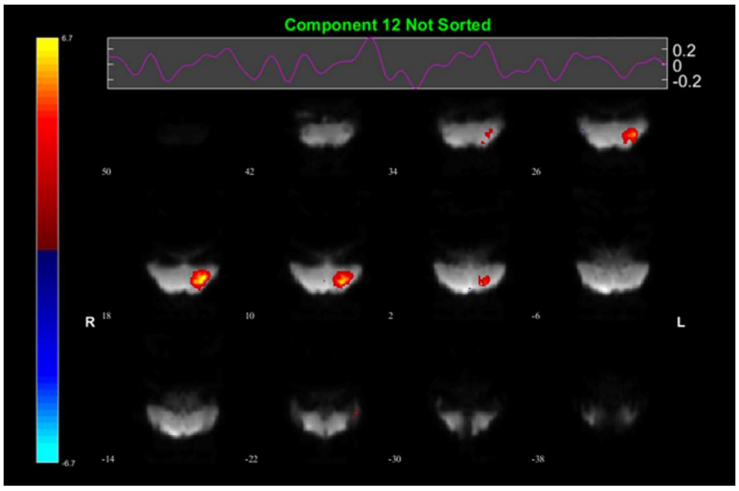

Component 12: Nido-A-int-R

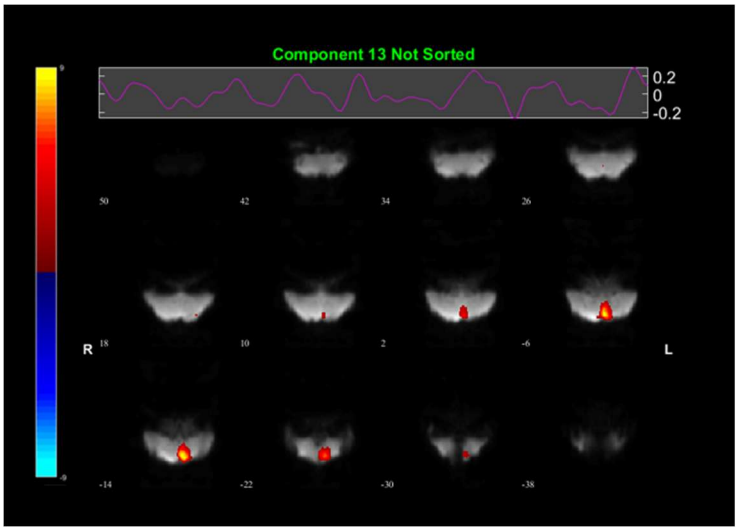

Component 13: NCM-R

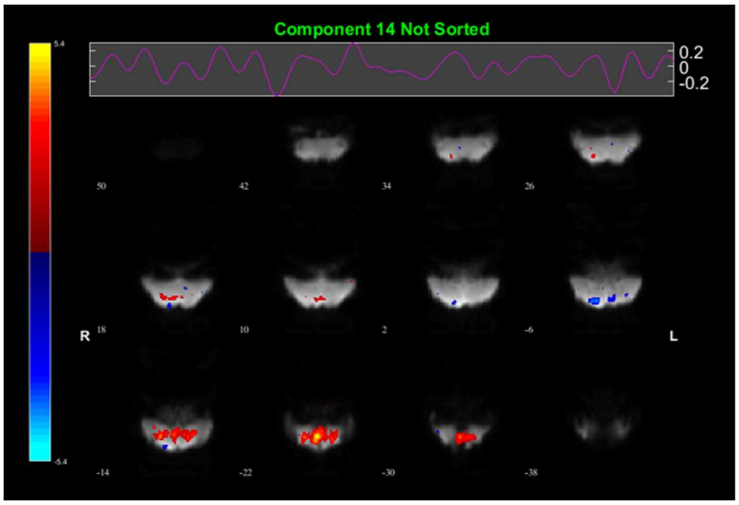

Component 14: Cerebellum + Nidopallium

This component was not included as a region because intensity is not as high as the other regions.

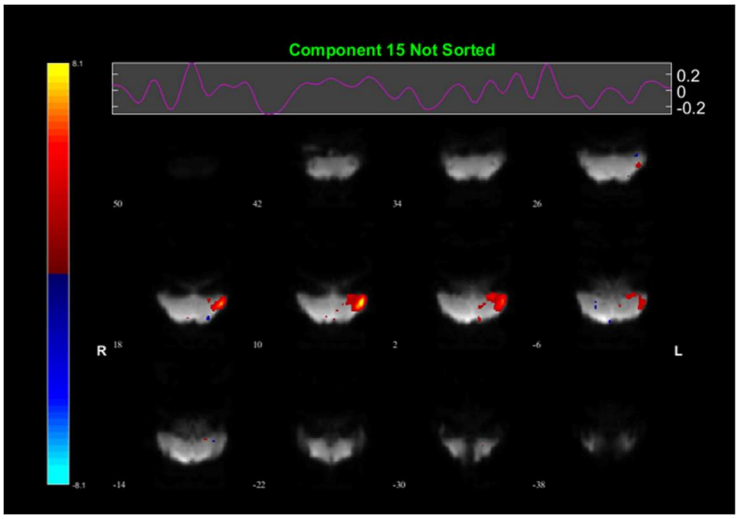

Component 15: Meso-PM-l-R

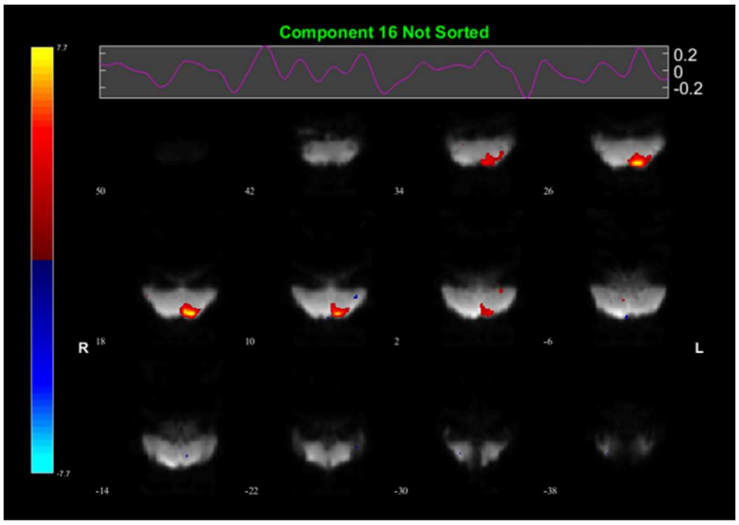

Component 16: Hyper-M-R

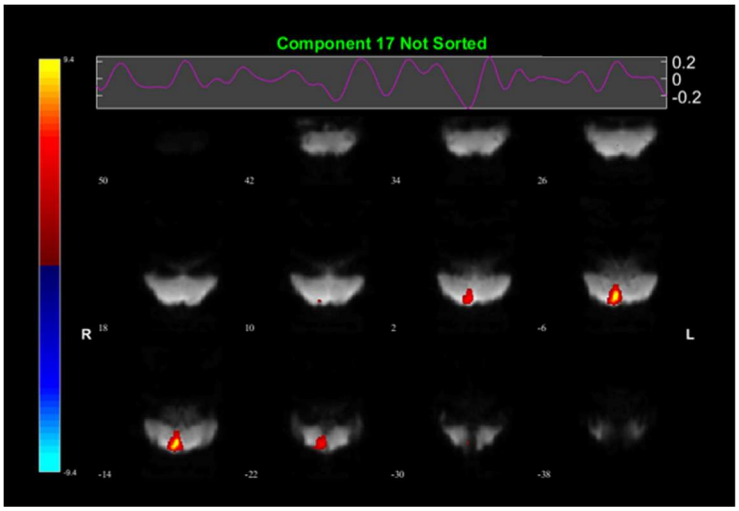

Component 17: NCM-L

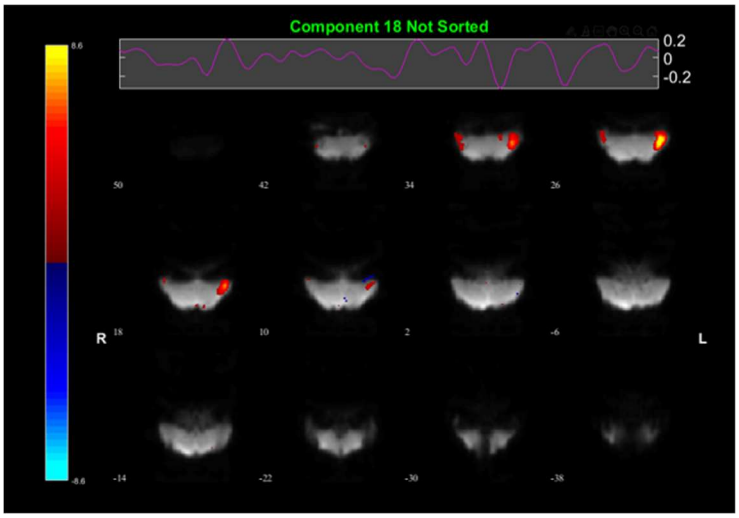

Component 18: Nido/meso-R

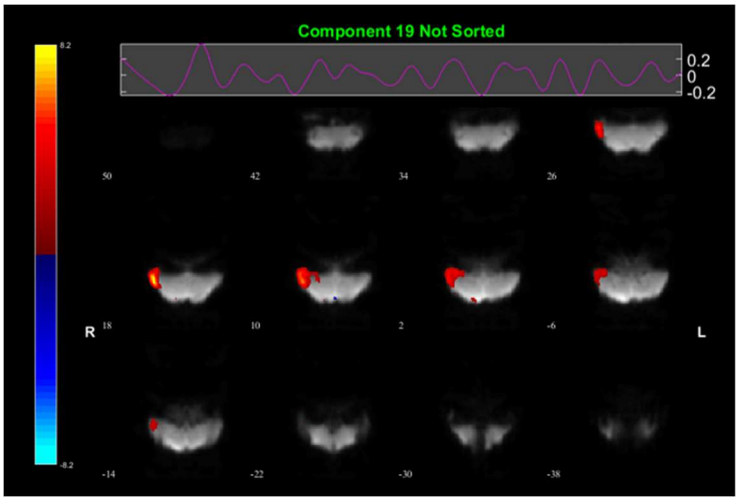

Component 19: Meso-A-I-L

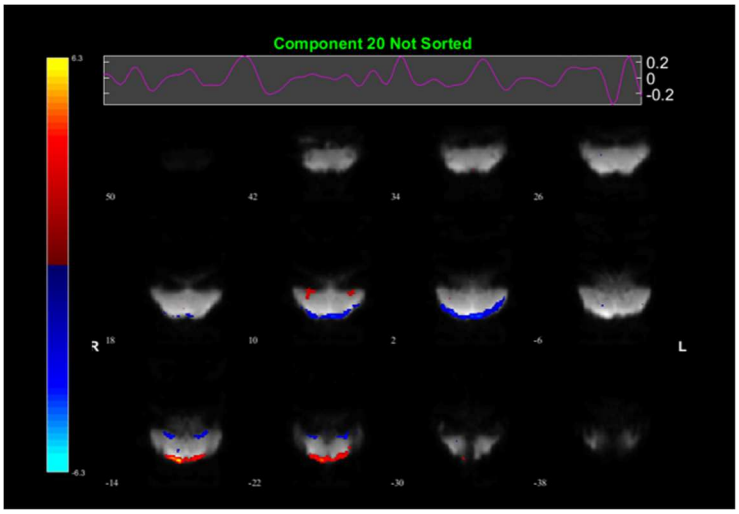

Component 20: Hippocampus

(+ anticorrelation Hyperpallium)

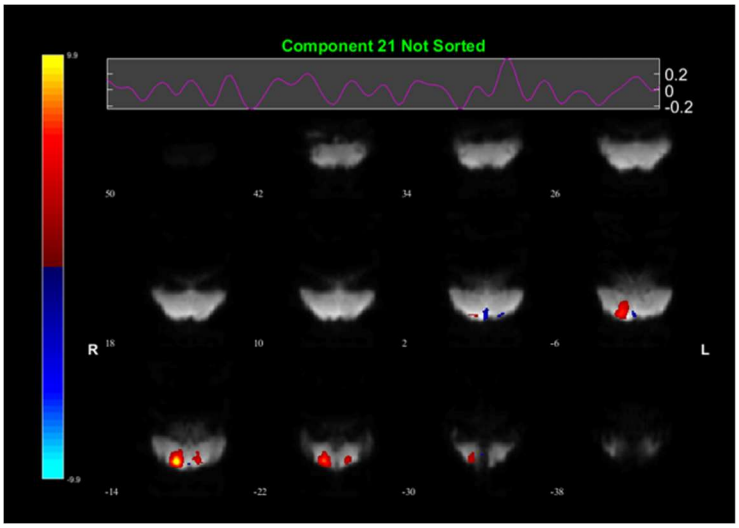

Component 21: NCL-L

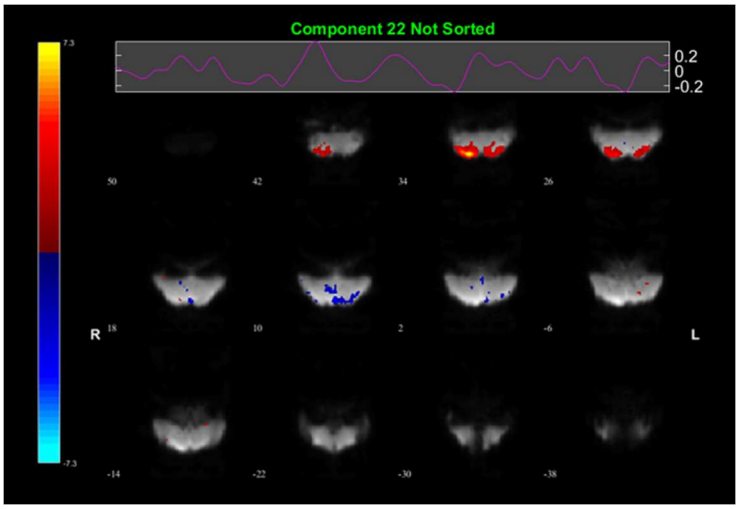

Component 22: Hyper-A-LR

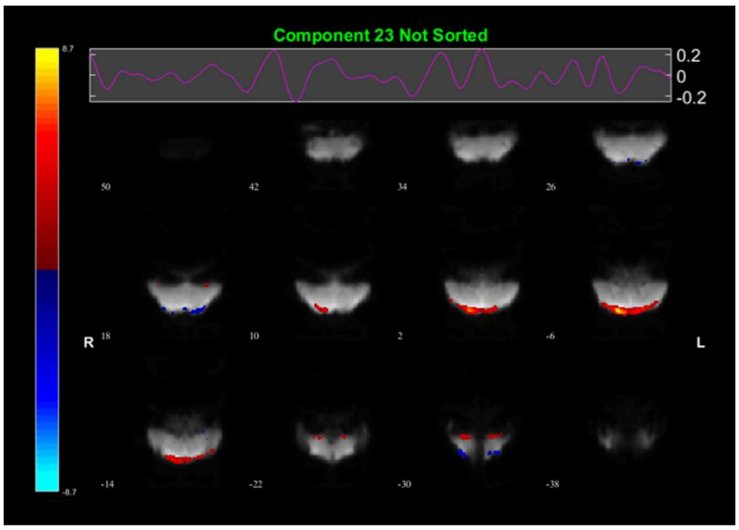

Component 23: Hyper-P-L

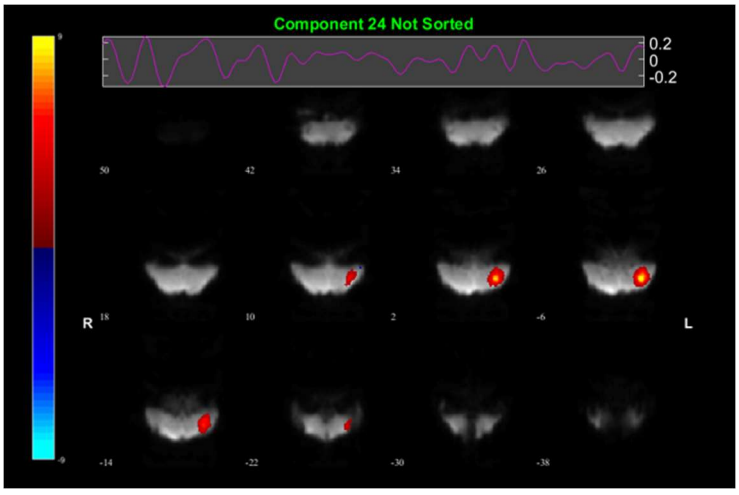

Component 24: Nido-P-int-R

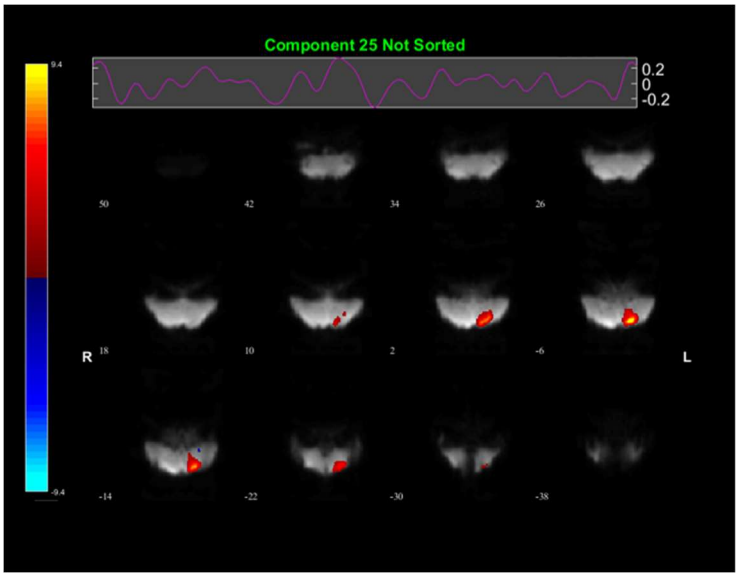

Component 25: NCL-R

Supplementary figure 1: 25 independent Components from all groups pooled together. The names beside the components are the regions later used in the functional connectivity matrices. The pictures show the bird brain from front to the back of the brain. The colourbar shows the intensity of the component. Warm colours signify a correlation or connection and cold colours signify an anti-correlation. The purple line on top is a timeseries showing how the pattern of activation changed over time

11.2 FC matrices

11.2.1 Full matrices (non-GSR)

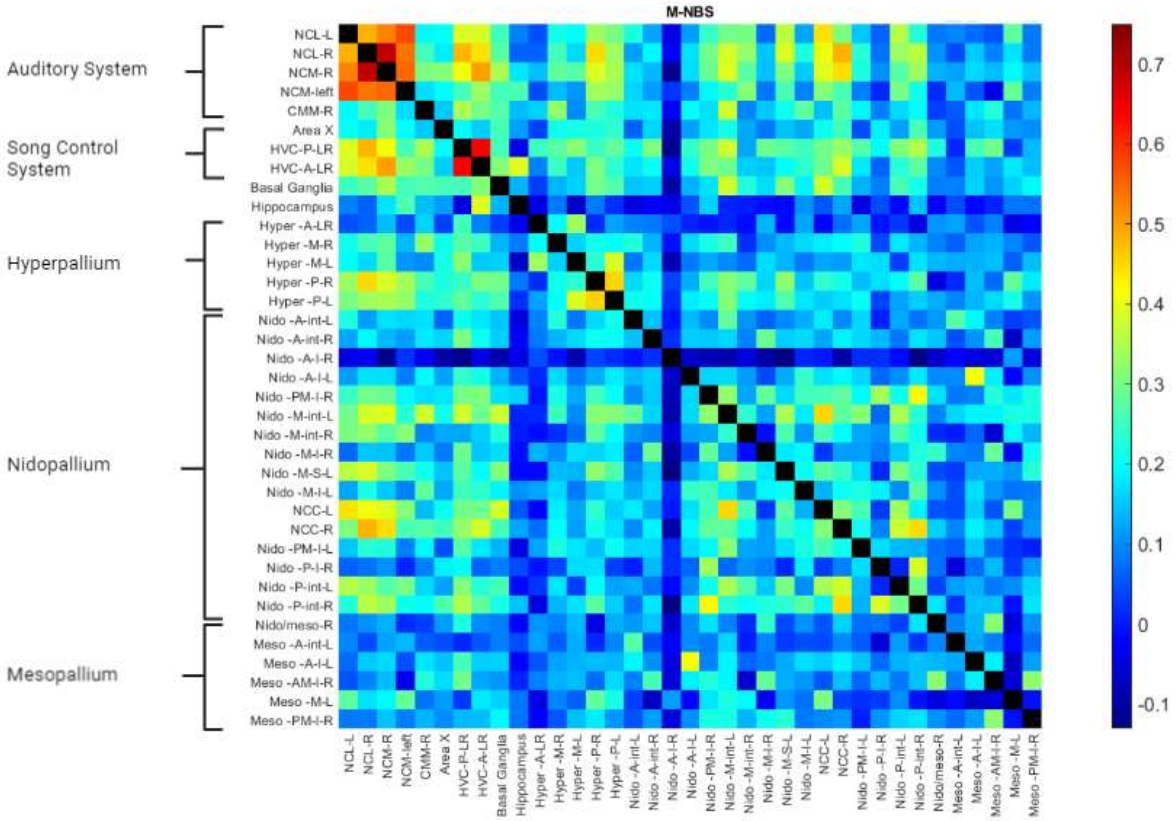

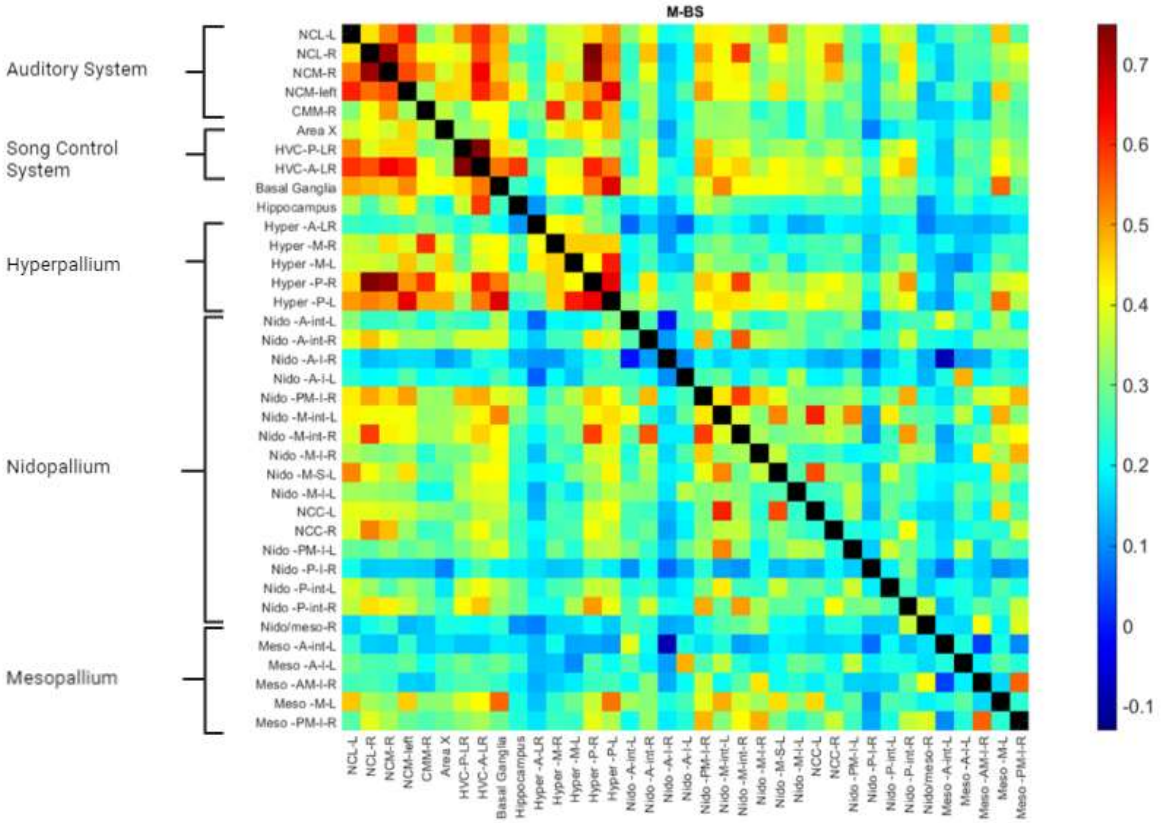
M-BS
Auditory System
Song Control System
Hyperpallium
Nidopallium
Mesopallium
NCL-L
NCL-R
NCM-R
NCM-left
CMM-R
Area X
HVC-P-LR
HVC-A-LR
Basal Ganglia
Hippocampus
Hyper -A-LR
Hyper -M-R
Hyper -M-L
Hyper -P-R
Hyper -P-L
Nido -A-int-L
Nido -A-int-R
Nido -A-I-R
Nido -A-I-L
Nido -PM-I-R
Nido -M-int-L
Nido -M-int-R
Nido -M-I-R
Nido -M-S-L
Nido -M-I-L
NCC-L
NCC-R
Nido -PM-I-L
Nido -P-I-R
Nido -P-int-L
Nido -P-int-R
Nido/meso-R
Meso -A-int-L
Meso -A-I-L
Meso -AM-I-R
Meso -M-L
Meso -PM-I-R
0.7
0.6
0.5
0.4
0.3
0.2
0.1
0
-0.1

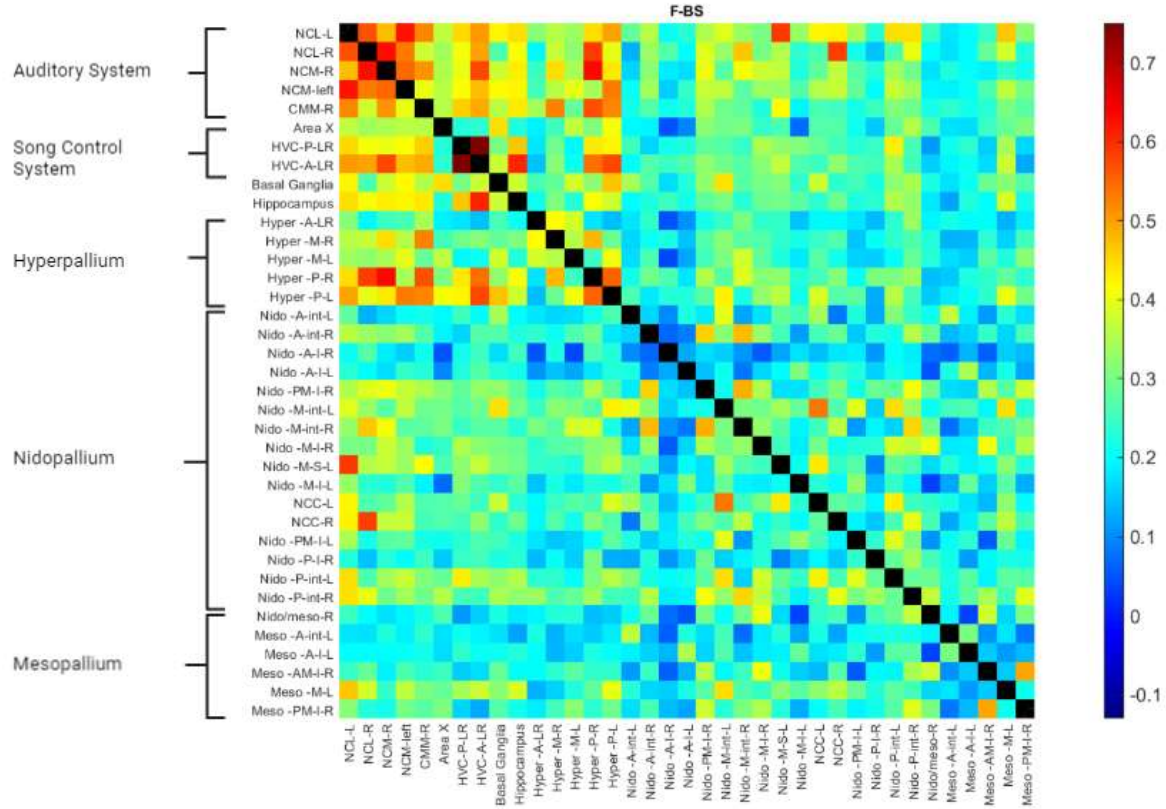
F-BS
Auditory System
Song Control System
Hyperpallium
Nidopallium
Mesopallium
NCL-L
NCL-R
NCM-R
NCM-left
CMM-R
Area X
HVC-P-LR
HVC-A-LR
Basal Ganglia
Hippocampus
Hyper -A-LR
Hyper -M-R
Hyper -M-L
Hyper -P-R
Hyper -P-L
Nido -A-int-L
Nido -A-int-R
Nido -A-I-R
Nido -A-I-L
Nido -PM-I-R
Nido -M-int-L
Nido -M-int-R
Nido -M-I-R
Nido -M-S-L
Nido -M-I-L
NCC-L
NCC-R
Nido -PM-I-L
Nido -P-I-R
Nido -P-int-L
Nido -P-int-R
Nido/meso-R
Meso -A-int-L
Meso -A-I-L
Meso -AM-I-R
Meso -M-L
Meso -PM-I-R
0.7
0.6
0.5
0.4
0.3
0.2
0.1
0
-0.1

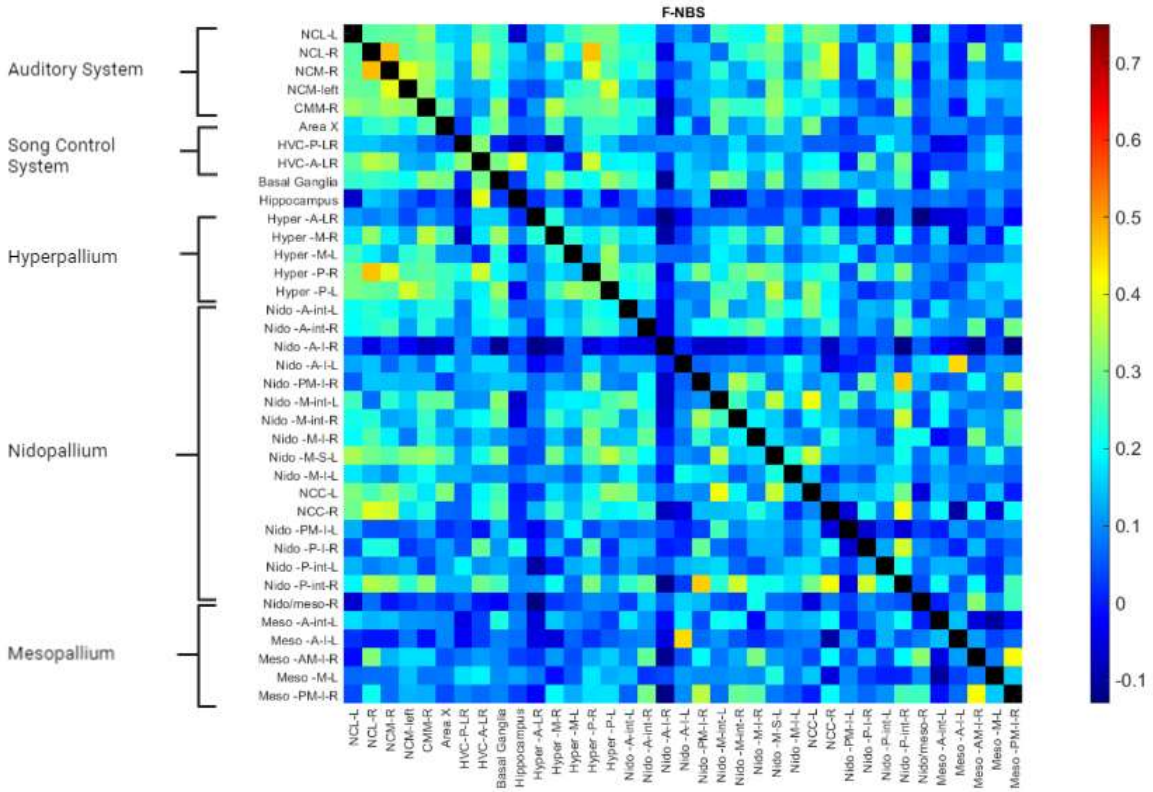

Supplementary figure 2: Full matrices with 37 regions from all 4 groups, M_BS, M_NBS, F_BS, F_NBS for non-GSR data. The values of the colour bar are based on the minimum and maximum values present in the matrices. Warm colours (red, yellow) represent positively connected regions and cold colours (blue) represent uncorrelated or anticorrelated connections.

11.2.2 Full matrices (GSR)

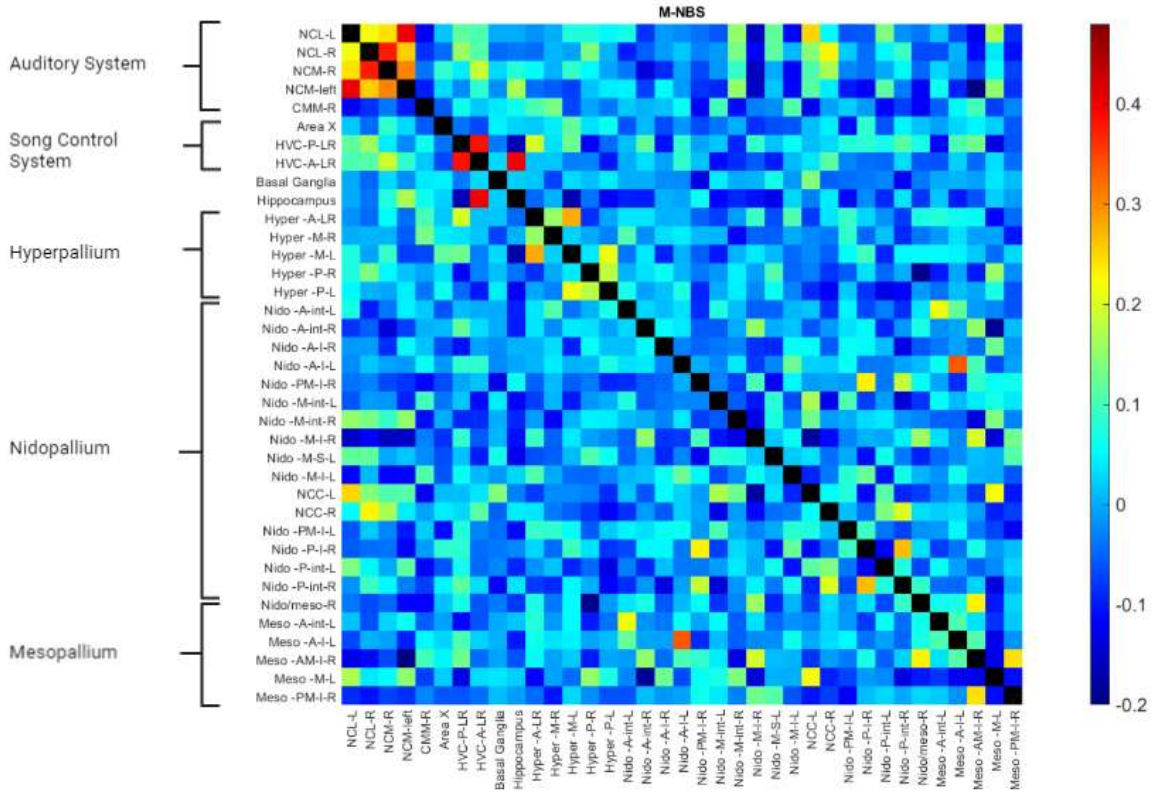

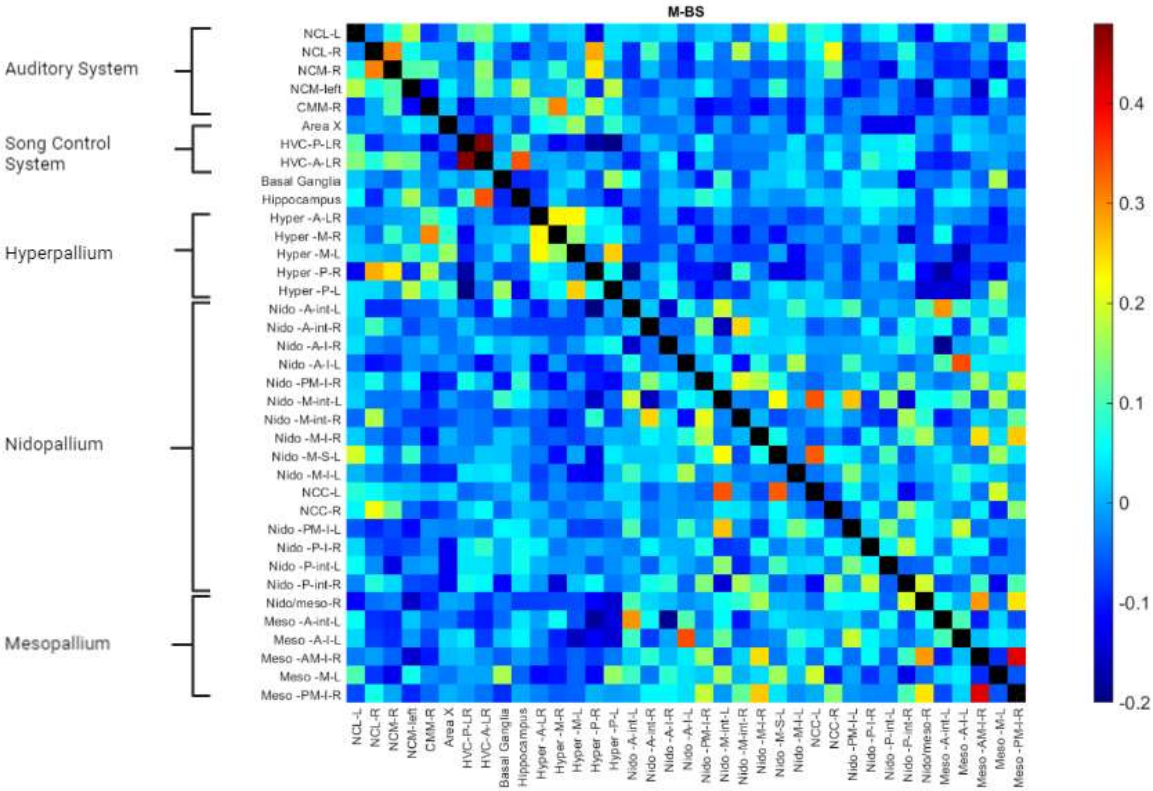

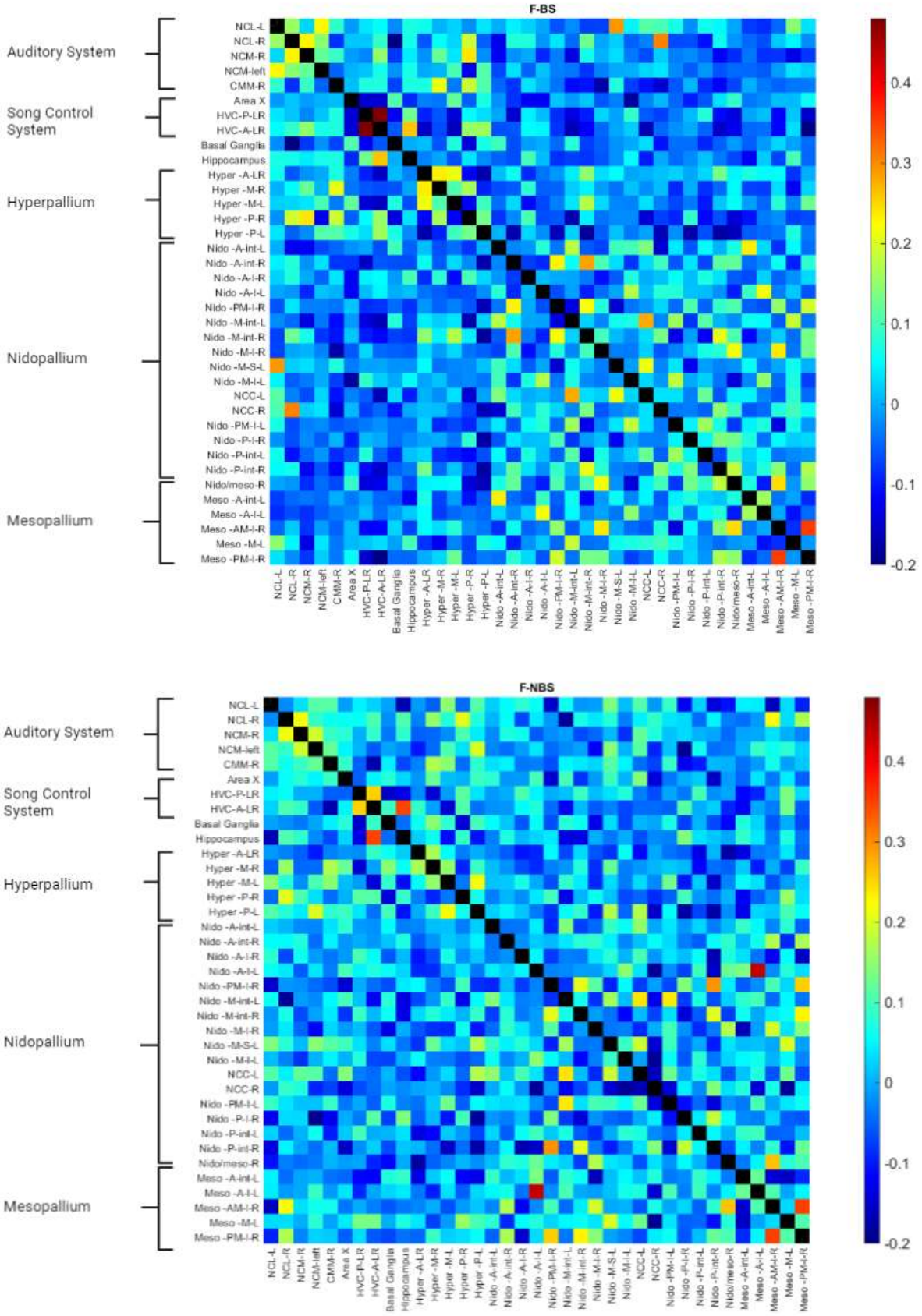

Supplementary figure 3: Full matrices with 37 regions from all 4 groups, M_BS, M_NBS, F_BS, F_NBS for GSR data. The values of the colour bars are based on the minimum and maximum values present in the matrices. Warm colours (red, yellow) represent positively connected regions and cold colours (blue) represent uncorrelated or anticorrelated connections.

11.3 Seed-based analysis

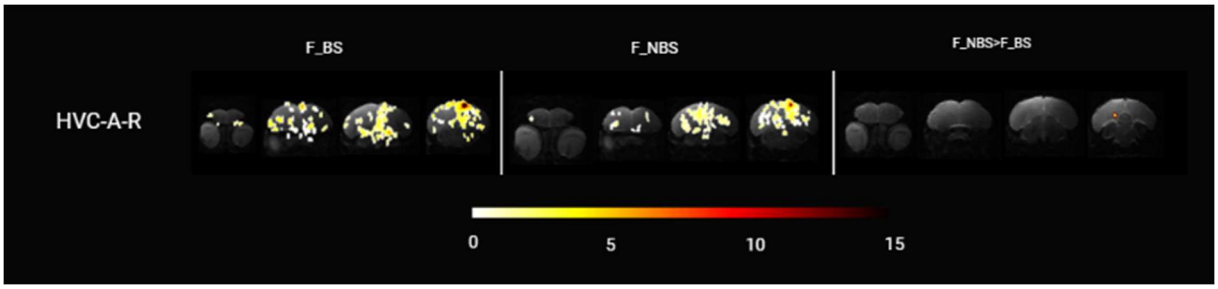

Supplementary Figure 4: Result of seed-based analysis without outlier, non-GSR, minimum 5 voxels cluster size and p <0.01 uncorrected. The first two columns are the results of the first level group level analysis of the females breeding season and non-breeding season (one-sample T-test). The last column shows the results of the second level seed-based analysis. (Two-sample T-test) It shows a difference in connection between HVC-A-R and RA that is more prominent in the non-breeding season.